AD NUMBER

AD468316

LIMITATION CHANGES

TO:

Approved for public release; distribution is unlimited.

FROM:

**Distribution authorized to U.S. Gov't. agencies and their contractors;
Administrative/Operational Use; AUG 1965. Other requests shall be referred to Air Force Arnold Engineering Development Center, Arnold AFB, TN.**

AUTHORITY

aedc ltr 6 dec 1965

AEF File

AEDC-TR-65-113

ADSORPTION OF HYDROGEN BY A THIN FILM OF TITANIUM

S. M. Kindall

ARO, Inc.

August 1965

AEROSPACE ENVIRONMENTAL FACILITY
ARNOLD ENGINEERING DEVELOPMENT CENTER
AIR FORCE SYSTEMS COMMAND
ARNOLD AIR FORCE STATION, TENNESSEE

NOTICES

When U. S. Government drawings specifications, or other data are used for any purpose other than a definitely related Government procurement operation, the Government thereby incurs no responsibility nor any obligation whatsoever, and the fact that the Government may have formulated, furnished, or in any way supplied the said drawings, specifications, or other data, is not to be regarded by implication or otherwise, or in any manner licensing the holder or any other person or corporation, or conveying any rights or permission to manufacture, use, or sell any patented invention that may in any way be related thereto.

Qualified users may obtain copies of this report from the Defense Documentation Center.

References to named commercial products in this report are not to be considered in any sense as an endorsement of the product by the United States Air Force or the Government.

ADSORPTION OF HYDROGEN BY A THIN FILM OF TITANIUM

S. M. Kindall
ARO, Inc.

FOREWORD

The research reported herein was sponsored by Arnold Engineering Development Center (AEDC), Air Force Systems Command (AFSC), Arnold Air Force Station, Tennessee under Program Element 61445014, Project 8951, and Task 895104.

The results of the research were obtained by ARO, Inc. (a subsidiary of Sverdrup and Parcel, Inc.), contract operator of AEDC under Contract AF 40(600)-1200 and ARO Project No. SW3417. The report was submitted by the author on May 5, 1965.

This report has been reviewed and is approved.

Harold L. Rogler
1st Lt, USAF
Aerospace Sciences Division
DCS/Research

Donald R. Eastman, Jr.
DCS/Research

ABSTRACT

Past experience has shown that the capture coefficient of a titanium surface for hydrogen is strongly dependent upon the surface temperature and the conditions under which the film is formed. This report presents the results of an investigation which determined the importance of some of the variables. It was found that the capture coefficient increased as the titanium surface temperature was decreased from 273 to 77°K. Moreover, the capture coefficient could be further increased by lowering the temperature of the substrate upon which the titanium film was deposited from 273 to 77°K. Also, the capture coefficient was found to be independent of film thickness and chamber pressure but increased when the deposition was carried out in an inert helium atmosphere. For the range of conditions investigated, the sticking fraction was found to vary from 0.01 to 0.5. The experimental data suggest that surface diffusion is an important part of the mechanism by which titanium captures hydrogen. Calculations using a theoretical model which incorporates diffusion agreed well with the experimental results.

CONTENTS

ILLUSTRATIONS

TABLES

NOMENCLATURE

A	Available adsorbent area, cm^2
A_o	Maximum adsorbent area, cm^2
$\hat{A}$	Constant of proportionality (frequency factor) in Arrhenius equation, sec^{-1}
a	Area of one site of adsorption, cm^2
C_1	Integration constant

C_H	Concentration of hydrogen just under titanium surface, molecules/cm^3
C_S	Maximum possible concentration of hydrogen in titanium (solubility) molecules/cm^3
D	Chamber diameter, cm
E	Activation energy for adsorption, Kcal/mole
E_a	Apparent or measured activation energy, Kcal/mole
H	Heat of adsorption, Kcal/mole
K	Ratio of rate constant to solubility
k	Rate constant (for diffusion), atoms/sec
L	Length of vacuum chamber, cm
ℓ	Liters
M	Molecular weight, gm
N	Total number of adsorption sites
n	Number of atoms
P	Instantaneous pressure, torr
P_1	Inflection point pressure - analogous with equilibrium pressure, torr
P_c	Cell pressure at any specific instant, torr
P_f	Forepressure, torr
P_o	Chamber base pressure, torr
Q	Throughput, torr-ℓ/sec
Q_{nL}	Throughput arriving at x = nL, torr-ℓ/sec
Q_{nL}^{AD}	Throughput adsorbed at x = nL, torr-ℓ/sec
Q_{nL}^{REFL}	Throughput reflected at x = nL, torr-ℓ/sec
q	Axial distance dependent throughput, torr-ℓ/sec
R	Universal gas constant, ergs/gm-mole-°K
S	Instantaneous pumping speed, ℓ/sec
S_o	Maximum pumping speed, ℓ/sec
T	Gas temperature in the vacuum chamber, °K

T_R	Room temperature, °K
t	Time, sec
V	Chamber volume, ℓ
x	Axial distance, cm
α	Sticking fraction
β	Exponential decay (of pumping speed) constant, sec
Δ	Incremental operator
θ	Fraction of surface coated with a monolayer
τ	Time of atom residence on titanium surface, sec

SECTION I
INTRODUCTION

To maintain a vacuum environment in space simulation chambers, an efficient pumping system is needed for each type of gas load generated. Cryosurfaces can be used effectively to pump most gases, but some gases such as hydrogen are especially difficult to cryopump and diffusion pumps are normally used to pump the hydrogen gas load. The use of titanium as an adsorption agent for hydrogen gas was investigated in an effort to find a more effective technique than cryopumping or diffusion pumping.

Titanium adsorbs hydrogen gas efficiently at pressures below the base pressure of most diffusion pumps. However, its usefulness for maintenance of a vacuum is determined by the rate at which it can adsorb hydrogen. References 1 and 2 indicate that the rate of adsorption varies with the technique employed. Thus, the experiments reported here were undertaken to determine the parameters which control the rate of adsorption. The parameters investigated were chamber pressure, film temperature, film thickness, substrate temperature during film deposition, and the influence of a low density inert gas atmosphere during deposition.

Experimental results are presented for sticking fraction and exponential decay constant as functions of temperature and pressure. With these results it is possible to compute the pressure versus time response of a vacuum chamber for a given gas load.

SECTION II
APPARATUS

2.1 VACUUM CHAMBER

The experiments were carried out in a cylindrical steel vacuum chamber, 10.4 in. in diameter by 10.5 in. long. The effective volume of this chamber, which includes some of the associated tubing connected to the chamber, was measured to be 16,585 ± 80 cm^3, and the effective surface area was calculated to be 3,307.8 cm^2. For nominal calculations, a volume of 16.6 ℓ and a surface area of 3.3×10^3 cm^2 were used. A schematic of the basic chamber arrangement is shown in Fig. 1.

The vacuum chamber was immersed in a temperature bath to control the chamber temperature. The base of the chamber was closed with a copper gasket seal, which was vacuum tight for cycling temperatures ranging from about 400 to 77°K provided care was taken to prevent large temperature gradients across the face of the seal.

2.2 PUMPING SYSTEM

The pumping system consisted of a single 90-ℓ/sec, air-cooled, oil diffusion pump backed by a roughing pump. The pump-out line joined the cell through a 2-in. elbow connected to the top of the chamber. The pumping speed obtained from the pumping system was measured to be 9.5 ℓ/sec for hydrogen and 2.5 ℓ/sec for nitrogen.

2.3 PRESSURE SENSOR SYSTEM

All data were read out in the form of a pressure-time response. The pressure was sensed with both a Bayard-Alpert ionization gage and a 90-deg magnetic sector partial pressure analyzer. Both types of gages were joined to a 16-in.-long, 1-in.-diam pipe which extended up and out of the temperature bath surrounding the vacuum chamber.

2.4 POROUS PLUG FLOW SYSTEM AND THROUGHPUT

Hydrogen was admitted to the chamber through a fritted glass porous plug as shown in Fig. 2. The conductance of the porous plug was measured in-place and at room temperature to be 1.1×10^{-3} ℓ/sec for hydrogen gas. The upper tolerable forepressure required for the porous plug to behave as a true molecular leak was above 300 torr, well above the forepressure range of 10 to 50 torr used during these experiments. Using P_f to denote the forepressure on the porous plug and P_c to denote the room temperature cell pressure, the throughput to the cell, Q, is given by

$$Q = (1.1 \times 10^{-3}\ \ell/\text{sec})(P_f - P_c) \qquad (1)$$

In these experiments, P_c was always negligible relative to P_f ($P_c < 10^{-4}$ torr and $P_f > 10$ torr). However, the low chamber temperature used for the experiments caused the throughput to the cell to be reduced. Using T_R to denote room temperature and T to denote cell temperature, the throughput to the cell is given by (Ref. 3):

$$Q = (1.1 \times 10^{-3}\ \ell/\text{sec})\ P_f\ \frac{T}{T_R} \qquad (2)$$

The value used for T_R was 298°K. Fluctuations about this value were not significant.

2.5 TITANIUM FILAMENTS

The titanium filaments were constructed of 8 to 10 strands of 20-mil tungsten wire around which 20-mil titanium wire was twisted to form a

neat sheath of titanium. The number of inches of titanium wire used was varied and is stated along with the experimental results. The ends of the tungsten strands were bolted to high current vacuum feedthroughs. No titanium made direct contact with the feedthroughs.

SECTION III
PROCEDURE

The cell was first pumped down at room temperature up to and through the fritted glass leak. Next, the temperature bath container was filled with the desired bath. Three bath temperatures were used. The first bath was liquid nitrogen at 77°K, the second bath was packed dry ice at 195°K, and the third was an ice water bath at 273°K. No attempt was made to obtain additional temperature baths because it was desired only to determine whether or not the rate of adsorption changed with temperature, and if so, in what direction.

After the first bath temperature was established, the gas addition line was isolated from the system; and a filament was evaporated by sending 120 amp through the filament (the current value at which evaporation began) and slowly increasing the filament current until burnout resulted. Next, the first bath was drained (if, as was the usual case, the rest of the experiment was to proceed at a different temperature), and the temperature bath container was filled with a different medium. During this temperature change time, which required from one to two hours, the gas addition system was purged with hydrogen, and a regulated hydrogen pressure of from 10 to 50 torr was established behind the flow valve.

Next, the flow valve was opened, and the pressure-time response in the cell was recorded. The diffusion pump was usually left open to the system during a run. The maximum pumping speed of 9.5 ℓ/sec contributed by the diffusion pump was negligible relative to the 10,000- to 30,000-ℓ/sec pumping speed obtained from the titanium deposit.

The bath temperature during titanium deposition, which was also the deposit substrate temperature, is hereafter referred to as the deposit temperature. Similarly, the bath temperature at which the experimental run was made and which was also the titanium film and gas temperature, is hereafter referred to as the run temperature. Originally, it was desired to run at each of the three bath temperatures (77, 195, and 273°K) for each one of the same three deposit temperatures. All of these runs were completed except a run at 273°K after deposition at 195°K. Three other types of runs were made. In the first run the deposit thickness

was changed, in the second the hydrogen gas pressure (i.e., the throughput) was changed, and in the third the titanium was deposited in a helium atmosphere. Specific details of each run are given with the results.

SECTION IV
BASIC PRESSURE RESPONSE AND THEORETICAL CONSIDERATIONS

The curvature of the resulting pressure-time response is indicative of the adsorption phenomenon and, as will be shown, the adsorption mechanism itself. An example of a typical pressure-time response for a hydrogen gas flow rate of 3.6×10^{-2} torr-ℓ/sec is shown in Fig. 3. In this case, the titanium was deposited at 195°K, and the data were taken while the chamber was immersed in a 195°K bath. The pressure response that would result if no titanium were present is shown in Fig. 3 as a dashed line. The presence of titanium adsorption maintains a chamber pressure in the 10^{-6} torr region (in this case) for about 3,000 sec. However, unlike the response of a conventional diffusion pump to a constant throughput, no equilibrium pressure is obtained from titanium adsorption. Instead, the pressure first rises as if it were going to approach asymptotically an equilibrium pressure but then proceeds to increase exponentially. This ensuing pressure rise is indeed exponential, as demonstrated in Fig. 4, where the same data are shown on a semilogarithmic scale. When the experiment is arranged so that the pressure in the exponential region rises faster than shown in Fig. 4, the almost horizontal region in Fig. 4 disappears as shown in Fig. 5. It can be seen in Fig. 5 that the exponential pressure increase extends through three decades of pressure. Also of interest in Fig. 5, and representative of the typical pressure-time response, is the return of the chamber pressure after gas flow termination to the initial chamber pressure. This particular behavior is not typical of general adsorption phenomena because of adsorption isotherms and thus influences the interpretation of the adsorption mechanism discussed later.

4.1 EXPONENTIAL DECAY CONSTANT

In terms of pumping speed, that is, rate of adsorption, the typical pressure response shown in Figs. 4 and 5 is that of an initial maximum pumping speed which proceeds to decay exponentially as the adsorption process continues. Thus, in order to complete the first objective of this study (to observe the behavior of rate of adsorption as the film temperature and deposition conditions are varied), it is necessary to observe both the initial pumping speed and the time constant of the exponential decay of pumping speed.

The decay of the pumping speed, S, from an initial value, S_o, can be empirically represented by

$$S = S_o \, e^{-\frac{t}{\beta}} \tag{3}$$

where β is defined to be the time constant in units of seconds. The reciprocal of the exponential term of Eq. (3) is, of course, the term which leads to the exponential pressure rise in Figs. 4 and 5. Thus the value of β can be determined directly from plots such as Figs. 4 and 5.

4.2 STICKING FRACTION

The sticking fraction associated with a pumping surface is defined as the fraction of molecules impinging on the surface per unit time that permanently adhere to the surface. If α denotes the sticking fraction, and the pumping speed associated with a pumping surface of area A is again denoted by S, then it follows from the definition of α that

$$S = \alpha \sqrt{\frac{RT}{2\pi M}} \, A \tag{4}$$

where the radical term is the Knudsen expression (in volumetric units) for the rate of gas impingement per unit area per unit time. In Eq. (4), R is the universal gas constant, T is the gas temperature, and M is the molecular mass of the gas species.

In a chamber to which a constant gas throughput, Q, is introduced while gas is being pumped out by a device with an associated constant volumetric pumping speed, S, the result is for the chamber pressure to increase up to a particular pressure value and then remain at this equilibrium pressure for the duration of gas flow. If P_e denotes the resulting equilibrium pressure and P_o denotes the initial chamber pressure, then it follows from conservation of mass that

$$Q = S(P_e - P_o) \tag{5}$$

Usually, to facilitate measurements, Q is made to be of such a size for any particular value of S that P_o is negligible relative to the resulting value for P_e. In this case it is possible to express S as

$$S = \frac{Q}{P_e} \tag{6}$$

In the case of titanium adsorption of hydrogen gas, no such equilibrium pressure exists. However, the equilibrium pressure to which the chamber approaches before the pressure proceeds to increase exponentially is apparent from the inflection suffered by the pressure-time

curve. Thus, using the inflection point pressure rather than an equilibrium pressure, it is possible to define the initial pumping speed, S_o. If P_1 is used to denote the inflection point pressure, then

$$S_o = \frac{Q}{P_1} \tag{7}$$

The initial sticking fraction, α, which will be referred to as just the sticking fraction for the remainder of this report, is then defined by

$$\frac{Q}{P_1} = \alpha \sqrt{\frac{RT}{2\pi M}}\, A \tag{8}$$

Equation (8) expresses a rather ideal situation where P_1 is uniform throughout the vacuum chamber. In any real chamber, this condition can never be exactly achieved. As can be seen in Fig. 1, the chamber geometry used here can contribute to a pressure gradient down the chamber since gas is introduced at one end and is continuously adsorbed as it passes down the chamber. What is needed, therefore, is a method of determining the pressure gradient and its influence on the measured value of P_1.

One method is to treat this problem in a manner similar to that used for conductance problems. The chamber is first considered to be a long circular pipe to obtain the pressure gradient attributable to conductance only. This gradient is then modified by the influence of adsorption at the chamber wall. Next, the end effects caused by adsorption and reflection at the chamber ends are included. From this, it is possible to express the pressure gradient down the chamber as a function of the chamber diameter and the sticking fraction. However, the gradient itself is not the main interest, and thus the gradient expression is solved for the specific length of this chamber. This introduces the admitted throughput, Q, and measured pressure, P_1, as boundary conditions. In a manner analogous to Eq. (8), the ratio of Q to P_1 is expressed as a function of all other variables. The complete derivation of this expression is given in the Appendix. The resulting expression is

$$\frac{Q}{P_1} = \alpha \sqrt{\frac{RT}{2\pi M}}\, \frac{\pi D^3}{4} \left\{ 1 + \sqrt{\frac{3}{\alpha}} \left[\frac{1}{1 + \sum_{n=1}^{\infty} e^{-2n\sqrt{3\alpha}\,L/D} \left(1 + \frac{\sqrt{3\alpha}}{4}\right)^{2n}} \right] - \left[\frac{\sum_{n=1}^{\infty} e^{-2n \frac{\sqrt{3\alpha}}{D} L} \left(1 - \frac{\sqrt{3\alpha}}{4}\right)^{2n-1}}{1 + \sum_{n=1}^{\infty} e^{-2n\sqrt{3\alpha}\,L/D} \left(1 - \frac{\sqrt{3\alpha}}{D}\right)^{2n}} \right] \right\} \tag{9}$$

where α is the sticking fraction, D is the chamber diameter, and L is the chamber length.

Normally, rarefied gas dynamics expressions are kept in the volumetric system in order to have a minimum of pressure dependent terms. In the case of Eqs. (8) and (9), the problem is not one of pressure dependence but temperature dependence. In order to plot the two equations, Q was transferred from torr-ℓ/sec to number of molecules per second, and P_1 was transferred from torr to number of molecules per second per square inch which impinge on a surface at P_1. Thus, P_1/Q was transferred from $(\ell/\text{sec})^{-1}$ to $(\text{in.}^2)^{-1}$. Plots of both Eqs. (8) and (9) are shown in Fig. 6 for the range of α from 0.01 to 1. These same two curves are repeated in Fig. 7 slightly more magnified for the range of α from 0.1 to 1. A sketch of the complete behavior of both equations showing two cross-over points is given in Fig. 15d.

Despite the necessary assumptions used to derive Eq. (9), this equation is believed to be a more accurate representation of the dependence of the ratio Q/P_1 on α for this particular chamber because it considers the actual situation. The idealized Eq. (8), on the other hand, is obviously much simpler to evaluate. Fortunately, most of the data occurs near the second cross-over point of the two curves. The values of sticking fraction for which the difference in evaluation between Eqs. (8) and (9) is significant are given into Tables I and II where both values are given.

SECTION V
RESULTS

The variation of sticking fraction for run temperatures of 77, 195, and 273°K is shown in Fig. 8. Each data point in Fig. 8 was taken from a separate pressure-time response, such as shown in Fig. 3. In each case, 80 in. of 20-mil titanium wire was evaporated and assumed to form a uniform film over the entire inner surface of the vacuum chamber. Three titanium deposit temperatures were used as indicated in Fig. 8, and hydrogen gas was admitted to the chamber at the rate of 7.24×10^{-2} atm-cc/sec for all three runs. The sticking fraction was determined from Eq. (8) using (after correcting for thermal transpiration) the inflection point pressure as discussed in Section 4.2. The dashed lines in Fig. 8 are not intended to represent the functional dependence of sticking fraction on run temperature but serve instead to emphasize the trend of the data.

It can be seen in Fig. 8 that, for all three deposit temperatures, the sticking fraction decreases as the run temperature increases, but the rate of decrease itself decreases as the deposit temperature increases. Thus, the three trend lines cross. This suggests that some particular run temperature exists such that for run temperatures above this value the sticking

fraction increases with increasing deposit temperature, and below this run temperature the sticking fraction decreases with increasing deposit temperature.

Figure 9 shows the same data presented in Fig. 8 except that the sticking fraction is plotted as a function of deposit temperature for each of the three run temperatures. Once again, dashed lines are used to represent the trends of the data. It can clearly be seen in Fig. 9 that the above-mentioned particular run temperature occurs in the neighborhood of 195°K.

Variations of exponential decay constant (defined in Section 4.1) with both run temperature and deposit temperature are shown in Fig. 10. In each case, the value of β was taken from experiments in which 80 in. of 20-mil titanium wire was evaporated and hydrogen gas admitted at the rate of 7.24×10^{-2} atm-cc/sec. At this flow rate, it was not possible to obtain data for a run temperature of 77°K. It can be seen in Figs. 10a and b that the data trends toward smaller values for the reciprocal of β as the run temperature increases. A smaller value for the reciprocal of β means that the pressure-time response takes longer to increase through any given increment of pressure above the inflection point pressure.

Thus, the general results presented in Figs. 8, 9, and 10 are that the highest initial sticking fractions are obtained at the lower run temperatures, but the longer periods of vacuum maintenance are obtained at the higher run temperatures.

The variation of sticking fraction with deposit thickness is given in Fig. 11a. In this series of experiments, six filaments, each containing 20 in. of 20-mil titanium wire, were evaporated. In this way, the first data point was obtained from a run using a film thickness corresponding to the deposition of 20 in. of titanium wire, the second data point was obtained from a run using two first film thicknesses deposited successively rather than simultaneously, and the third data point was obtained from a run using three first film thicknesses deposited successively. This sequential mode of evaporation lessened the possibility of a change in deposit density which might occur if all the titanium were deposited over the same area in the same time increment.

A severe decrease in the measured value of sticking fraction is discernible in Fig. 11a. That is, the normal value for α that was obtained when depositing at 195°K and running at 195°K was about 0.1 (see Fig. 9), whereas the average value in Fig. 11a is slightly less than 0.04. The reason for this decrease is not immediately clear. One possible explanation is that the sequential mode of evaporation of several filaments resulted

in an increase in the ratio of tungsten to titanium in the deposit, thus reducing the exposed titanium. Despite this unwanted effect, Fig. 11a indicates that the sticking fraction of titanium for hydrogen gas is independent of film thickness for the thicknesses used in this study.

The variation of the reciprocal of the exponential decay constant with deposit thickness is given in Fig. 11b. The first three data points in Fig. 11b (i.e., 20, 40, and 60 in.) were obtained from the three runs represented in Fig. 11a. Considering these three points only, there appears to be no significant dependence of exponential decay constant on deposit thickness. The data point at 80 in. of titanium represents the normal 80-in. filament for a deposit temperature of 195°K and a run temperature of 195°K (see Fig. 10c, where $\beta^{-1} = 10.5 \times 10^{-4}$ sec^{-1}), and the data point at 100 in. was taken from one of the preliminary runs of this study at the same deposit and run temperatures. The sticking fractions measured for the two runs represented by these last two data points were both about 0.1. Thus, in these cases, a change in sticking fraction occurred without a change in exponential decay constant while the run temperature and deposit temperature were maintained constant through the series of runs. Because a variation in sticking fraction is not necessarily reflected in the exponential decay constant, this implies that the sticking fraction and exponential decay constant are fundamentally independent--related possibly only parametrically through such parameters as temperature and deposit density.

Clausing (Ref. 2) showed that a large increase in sticking fraction of titanium for hydrogen and other gases could be obtained by depositing the titanium in an atmosphere of helium. In order to investigate this, runs were made at 195°K in which the deposit was formed also at 195°K but at different helium pressures. A flow rate of 7.24×10^{-2} atm-cc/sec was again used for each run, and Eq. (8) was applied to each inflection point pressure to obtain the sticking fraction. The results of this series of runs are shown in Fig. 12.

The principal advantage of increasing the sticking fraction of 195°K titanium by depositing in a helium atmosphere is that 195°K titanium also possesses a moderately low value for the reciprocal exponential decay constant (see, for example, Fig. 10). However, it is found that the pressure response attributable to adsorption by a film deposited under such conditions no longer exhibits a pure, exponential pressure rise. This is demonstrated in Fig. 13 which shows the pressure-time response obtained from adsorption by titanium deposited at 195°K in a 1.5×10^{-2} torr atmosphere of helium. The run temperature was also 195°K and the usual flow rate of 7.24×10^{-2} atm-cc/sec of hydrogen gas was admitted to the chamber. The dashed line in Fig. 13 is a translation of the straight line in Fig. 4 (same experimental conditions) which demonstrates the deviation of the response in Fig. 13 from the expected pure exponential increase in pressure.

The variation of sticking fraction with chamber pressure is shown in Fig. 14. In this case, the titanium was deposited at 195°K and the run was made at 195°K, but the flow rate of hydrogen gas was periodically changed to obtain a range of inflection point pressures corresponding to the range of flow rates. As can be seen in any one of the pressure-time responses in this report, the time available for determining an inflection point pressure is relatively short. Thus it was necessary in this series of runs to evaporate another filament (80 in. of titanium) every few hundred seconds or whenever the chamber pressure showed signs of beginning to rise exponentially. To prevent the chamber temperature from changing because of these in-run evaporations, each evaporation was accomplished as quickly as possible.

Once again a slight decrease in sticking fraction occurred, this time from the usual value of 0.1 to an average of 0.076. The assumption that this effect is caused by an over-abundance of tungsten in the deposit was more apparent in this case because this process of rapid evaporation resulted in an increase in the amount of tungsten evaporated per filament. This was determined from observation of burned filaments at the conclusion of this experiment. However, this additional masking was maintained fairly uniformly throughout the series of measurements. As can be seen in Fig. 14, there is no indication of a dependence of sticking fraction on chamber (hydrogen) pressure for a range extending from 4×10^{-7} torr to 1.35×10^{-5} torr.

SECTION VI
DISCUSSION

In attempting to ascertain a mechanism of adsorption compatible with the results of these experiments, it becomes apparent that more than one mechanism is suggested. The results obtained in this study, plus the results obtained by other investigators, suggest that the hydrogen molecules are initially attracted to the titanium surface by adsorption forces where they are dissociated into atoms and contained on the surface for a time, τ, after which the atoms diffuse into the titanium. Each atom that diffuses into the titanium re-opens a site for surface adsorption. Thus, the initial sticking fraction, α, is determined by the rate of adsorption, but the ensuing decay in pumping speed, as expressed by Eq. (3), is controlled by a decay in rate of diffusion.

There are two reasons for proposing diffusion as part of the total mechanism. First, hydrogen is known to readily diffuse into some metals (see, for example, Ref. 4). But second and more important, the

absence of an adsorption isotherm (Ref. 5) as indicated by no apparent change in chamber base pressure after an extended period of adsorption (see Fig. 5) can be explained only in terms of a mechanism such as diffusion whereby atoms are removed from the adsorbent surface.

6.1 INDICATED TYPE OF ADSORPTION

It will be suggested here that the results of these experiments indicate physical adsorption. Physical adsorption is a process in which the adsorbed molecules are bound to the adsorbent surface by Van der Waal type forces as opposed to chemisorption in which the surface bonds are similar to chemical forces. The argument for physical adsorption is taken from the measured value of activation energy and the temperature dependence of the rate of adsorption.

As indicated in Fig. 14, the volumetric rate of adsorption is independent of pressure. This means that the rate at which molecules are adsorbed is directly proportional to pressure. It is desirable in this discussion to replace pressure with its equivalent in number of molecules in the chamber. Thus the above statement can be expressed as

$$\left(\frac{dn}{dt}\right)_{ad} = kn \tag{10}$$

where $(\frac{dn}{dt})_{ad}$ denotes the rate of adsorption of molecules and n denotes the number of molecules in the chamber. The constant, k, in Eq. (10) is known as the rate constant. Inserting the ideal gas law into Eq. (10) yields

$$k = \frac{S}{V} \tag{11}$$

where S is the volumetric pumping speed and V is the chamber volume.

The rate constant is related to the apparent (in this case, the measured) activation energy by the well-known Arrhenius equation (see for example Ref. 6, page 546),

$$k = \hat{A}\, e^{-\frac{E_a}{RT}} \tag{12}$$

where E_a is the apparent activation energy as defined below, R is the universal gas constant, T is the absolute temperature, and $\hat{A}$ is a constant generally designated as the frequency factor. The apparent activation energy is actually the difference between the true activation energy and the heat of adsorption. That is,

$$E_a = E - H \tag{13}$$

where E is the true activation energy and H is the heat of adsorption. (For a complete discussion of this point, see page 546 of Ref. 7).

Now, inserting Eqs. (11) and (13) in Eq. (12) gives

$$\frac{S}{V} = \hat{A}\, e^{-\frac{E-H}{RT}} \tag{14}$$

Using data from Fig. (8), i.e., $\frac{S_1}{S_2} = 2.24$, $T_1 = 77°K$ and $T_2 = 273°K$, the calculated value for $|E - H|$ is 170 cal/mole. The values of $|E - H|$ that can be determined from the rest of the data from Fig. 8 range about the same order of magnitude. Thus the indicated value for E is nearly the same as for H. Values of H for titanium adsorption of hydrogen have not been measured. However, using the assumption that physical adsorption is indicated by low values for the apparent activation energy (i.e., low as compared to 10^4 to 10^5 cal/mole, page 463 Ref. 7), then the above calculation indicates that physical adsorption controls the initial phase of the adsorption process.

Probably the most decisive indication of physical adsorption is the measured decrease in rate of adsorption with an increase in film temperature (see Fig. 9). This is opposed to the behavior associated with surface chemisorption in which the rate of adsorption increases with an increase in film temperature (Ref. 5).

6.2 DIFFUSION

The long sustained periods of adsorption such as shown in Figs. 3 and 5 indicate that either very thick multi-layers of hydrogen build up on the film surface or the adsorbed atoms diffuse on into the titanium film. The hypothesis presented here is that diffusion does occur; and from this hypothesis, it will be shown that the expected pressure-time behavior caused by diffusion agrees with the measured behavior. Physically adsorbed atoms, incidentally, would be more likely to yield to diffusion than would more tightly bound chemisorbed atoms.

The proposed mechanism, then, is that hydrogen molecules strike the titanium surface where they have a probability, α, of remaining attached to the titanium surface. The attached molecules dissociate (Refs. 8 and 9) and remain on the titanium surface as adsorbed atoms for an average time, τ, after which they begin to diffuse into the titanium lattice structure. It is important to note that τ, in this case, is not the usual residence time associated with gas molecule-surface interactions but is instead a time of delay between adsorption and diffusion. In the following development of the result of diffusion on the pumping speed of the titanium film, it has been assumed that τ is greater than the time required to form a monolayer.

The rate at which hydrogen diffuses into a metal, $\left(\frac{dn}{dt}\right)_{Dif}$, is expressed by (see page 179 of Ref. 10)

$$\left(\frac{dn}{dt}\right)_{Dif} = k\,\theta\left(1 - \frac{C_H}{C_S}\right) \tag{15}$$

where k is the rate constant, θ is the fraction of the titanium surface covered by hydrogen atoms, C_H is the concentration of hydrogen just inside the metal, and C_S is the concentration of hydrogen inside the titanium when saturated.

The values for C_H and C_S can be expressed as

$$C_H = \int_0^t \left(\frac{dn}{dt}\right)_{Dif} dt \tag{16}$$

$$C_S = \int_0^\infty \left(\frac{dn}{dt}\right)_{Dif} dt \tag{17}$$

And, as previously stated, the value of θ is unity. Therefore, the following is obtained from Eq. (15):

$$\left(\frac{d^2n}{dt^2}\right)_{Dif} = -K\left(\frac{dn}{dt}\right)_{Dif} \tag{18}$$

where

$$K = \frac{k}{\int_0^\infty \left(\frac{dn}{dt}\right)_{Dif} dt} \tag{19}$$

Solving Eq. (18) gives

$$\left(\frac{dn}{dt}\right)_{Dif} = C_1\, e^{-Kt} \tag{20}$$

where C_1 is a constant of integration.

Now, if N denotes the total number of adsorption sites on the titanium surface and a denotes the area of a site, defined such that the titanium surface area, A_o, is given by

$$A_o = Na \tag{21}$$

then the rate of change of area available for adsorption is given by

$$\frac{dA}{dt} = \left(\frac{dn}{dt}\right)_{Dif} a = a\,C_1\, e^{-Kt} \tag{22}$$

which when integrated and constrained by the boundary conditions that $A = 0$ at $t = \infty$ and $A = A_o$ at $t = 0$, reduces to

$$A = A_o\, e^{-Kt} \tag{23}$$

Referring now to Eq. (4), it follows that

$$S = \alpha \sqrt{\frac{RT}{2\pi M}}\ A_o\ e^{-Kt} = S_o\ e^{-Kt} \tag{24}$$

Thus, the behavior predicted by diffusion satisfies the empirical Eq. (3).

The influence of a decaying diffusion rate on the pressure-time response can be determined directly from Eq. (5). That is,

$$Q = S\,(P - P_o) \tag{25}$$

From this equation it follows that

$$P = \frac{Q}{S_o}\ e^{K(t-\tau)} + P_o \tag{26}$$

where the time is now expressed by $(t - \tau)$ to acknowledge the difference between initiation of gas flow at $t = 0$ and initiation of diffusion at $t = \tau$. As a natural consequence of having neglected the transient behavior of diffusion, it is now necessary to define

$$t - \tau = 0 \quad \text{for} \quad t < \tau \tag{27}$$

A more complete version of Eq. (26) can be obtained by observing the time dependence resulting from adsorption only. This can be obtained quite simply by neglecting diffusion for the moment and equating the rate of appearance of mass into the chamber to the difference between the rate of gas flow and the rate of adsorption.

That is,

$$V\ \frac{dP}{dt} = Q - S_o\,(P - P_o) \tag{28}$$

Integrating Eq. (28) gives

$$P = \frac{Q}{S_o}\left(1 - e^{-\frac{S_o}{V}t}\right) + P_o \tag{29}$$

Combining Eqs. (29) and (26) gives

$$P = \frac{Q}{S_o}\left(1 - e^{-\frac{S_o}{V}t}\right) e^{K(t-\tau)} + P_c \tag{30}$$

which by observation expresses pressure-time behaviors such as Figs. 3, 4, and 5 quite well. Thus by hypothesizing diffusion, the correct pressure-time response can be derived.

6.3 EXPONENTIAL DECAY CONSTANT

By comparing Eqs. (3) and (24), it can be seen that K is the reciprocal of the exponential decay time constant. Thus, Fig. 10 can be thought of as

plots of the variation of K with run temperature and deposit temperature. The physical interpretation of K is given by Eq. (19). The integral term of Eq. (19) is actually nothing more than the solubility of hydrogen in titanium. Thus

$$K = \frac{\text{rate constant}}{\text{solubility}} \tag{31}$$

and, as can be seen in Fig. 10, this ratio decreases with increasing run temperature. The reason for a decrease in K with run temperature is believed to be the result of increasing solubility of hydrogen in titanium with increasing titanium temperature. Unfortunately, data taken on the solubility of hydrogen in titanium (page 538, Ref. 11) shows that for $T > 300°K$, the solubility decreases with temperature. There is a good possibility, however, that the solubility of hydrogen in titanium is a maximum at some temperature near room temperature such that the solubility increases with temperature below room temperature. Such a behavior could account for the difference in behavior between low temperature and high temperature titanium adsorption of hydrogen. Radical changes in the behavior of solubility with temperature are not uncommon. The solubility of oxygen in silver, for example, undergoes a minimum near 400°K (see page 155, Ref. 8).

On the other hand, the indicated decrease in K with increasing deposit temperature, as shown in Fig. 10, probably results from a decrease in rate constant caused by an increase in titanium density. It is known that higher substrate temperatures during deposition yield shinier deposits. This indicates that the deposit surface is smoother at higher deposit temperatures which implies that the deposited atoms have more mobility on warmer substrate surfaces--sufficient mobility to form a smooth surface and thus also (possibly) pack closer together.

The change caused by depositing the titanium in a helium atmosphere is more difficult to interpret. It is believed that the helium atmosphere causes the titanium to be porous, resulting in greater surface area and thus increasing the rate of adsorption which is measured as an increase in sticking fraction and contributing capillary diffusion to the total process of gas removal.

SECTION VII
CONCLUSIONS

It can be concluded from this study that for run and deposit temperatures from 77 to 273°K:

1. The sticking fraction and exponential decay constant, as defined in this report, completely specify the pressure-time response obtained by using titanium adsorption to pump a constant rate of flow hydrogen gas load.
2. The sticking fraction of titanium for hydrogen decreases as the run temperature (titanium film temperature) increases, but the rate of decrease itself decreases as the deposit temperature (substrate temperature during deposition) increases.
3. The sticking fraction is independent of deposit thickness and chamber pressure.
4. The sticking fraction is increased by depositing the titanium in a helium atmosphere.
5. The reciprocal of the exponential decay constant decreases with an increase in both run temperature and deposit temperature.
6. The reciprocal of the exponential decay constant is independent of deposit thickness.
7. The mode of titanium adsorption of hydrogen appears to be physical adsorption.
8. Diffusion appears to be a principal mechanism in the total process by which titanium removes hydrogen gas.

APPENDIX
INFLUENCE OF CHAMBER GEOMETRY ON STICKING FRACTION

Let the variable x denote the axial distance down the chamber. The throughput transmitted through a circular pipe of diameter D and length L is given by (Ref. 12)

$$Q = \frac{\pi}{3}\sqrt{\frac{RT}{2\pi M}}\,\frac{D^3}{L}\,(\Delta P) \tag{I-1}$$

where ΔP is the difference in pressure (innately negative) from x = 0 to x = L and Q is the throughput. In differential form Eq. (I-1) can be expressed as

$$Q = -\frac{\pi}{3}\sqrt{\frac{RT}{2\pi M}}\,D^3\,\frac{dP}{dx} \tag{I-2}$$

In the case of ordinary transmission, Q is the same for any value of x, but in this case gas is being continuously adsorbed by the chamber walls. Therefore, there exists a change in Q with x. The symbol q will be used to denote the general x dependent value of throughput, Q with a subscript or superscript will denote a specific value of q, and Q with no subscript or superscript will denote the rate at which gas enters the system. From Eq. (I-2),

$$\frac{dq}{dx} = -\frac{\pi}{3}\sqrt{\frac{RT}{2\pi M}}\,D^3\,\frac{d^2P}{dx^2} \tag{I-3}$$

Now, the volumetric rate of adsoprtion by an incremental ring around the chamber of area dA (see Fig. 15a) is the product of the sticking fraction, α, times the volume of gas impinging on dA per unit time. If P is the pressure at x, then (recalling that by definition, $Q = P\frac{dv}{dt}$,

$$dq = -\alpha\sqrt{\frac{RT}{2\pi M}}\,P\,dA \tag{I-4}$$

and therefore

$$\frac{dq}{dx} = -\alpha\sqrt{\frac{RT}{2\pi M}}\,\pi D\,P \tag{I-5}$$

Equating Eqs. (I-5) and (I-3) gives

$$\frac{d^2P}{dx^2} = \frac{3\alpha}{D^2}\,P \tag{I-6}$$

which when solved (and a physically impossible extraneous root is discarded) gives

$$P = P_1\,e^{-\frac{\sqrt{3\alpha}}{D}x} \tag{I-7}$$

where P_1 is once again the measured pressure at x = 0.

A second useful expression can be obtained by taking the derivative of Eq. (I-5) and equating the resulting $\frac{dP}{dx}$ to the $\frac{dP}{dx}$ of Eq. (I-2). This gives

$$\frac{d^2q}{dx^2} = \frac{3a}{D^2}\, q \tag{I-8}$$

which when solved and given the same physical restriction as Eq. (I-6) to eliminate an extraneous root, gives

$$q = Q_o\, e^{-\frac{\sqrt{3a}}{D}x} \tag{I-9}$$

where Q_o is that part of Q which is not adsorbed at x = 0 (see Fig. 15b). A third useful expression can be obtained by differentiating Eq. (I-9) to obtain $\frac{dq}{dx}$ and equating this to Eq. (I-5) -- which when solved for P, gives

$$P = \frac{\sqrt{3a}}{D^2\pi a}\,\frac{Q_o}{\sqrt{\frac{RT}{2\pi M}}}\, e^{-\frac{\sqrt{3a}}{D}x} \tag{I-10}$$

Equation (I-10) is of particular use when q is known at some value of x, say x = a, and it is desirable to express P at x = b where b > a. Then

$$P_b = \frac{\sqrt{3a}}{D^2\pi a}\,\frac{Q_a}{\sqrt{\frac{RT}{2\pi M}}}\, e^{-\frac{\sqrt{3a}}{D}(b-a)} \tag{I-11}$$

The remainder of this derivation consists of mathematically tracing the behavior of Q as a single gas packet bounces back and forth through the chamber. Such a gas packet should, strictly speaking, be denoted by $Q\Delta t$. However, in the end it is desirable to return to a continuous flux which would require dividing by the same Δt. Thus the introduction of a time parameter is an unnecessary complication, and the packet will be symbolized by just Q.

In order to eliminate difficulties involved in considering a negative x direction, the chamber is stretched out so that only a positive x direction exists (see Fig. 15c). Now, of the initial packet entering the chamber, a part, Q_o^{AD}, is adsorbed immediately at x = 0 (see Fig. 15b). The remainder, Q_o, starts down the chamber. At the end of the chamber, i.e., at x = L, an amount Q_L arrives which is reduced from Q_o by the amount of adsorption suffered in travelling the length of the chamber. At x = L, an amount of gas, Q_L^{AD}, is adsorbed and the rest, Q_L^{REFL}, is reflected. The process continues until an insignificant amount of the initial packet remains. In order to obtain the total flux leaving the chamber end at x = 0, it is necessary to add $Q_o + Q_{2L}^{REFL} + Q_{4L}^{AD} + \ldots$ and the total flux adsorbed at x = 0 is given by $Q_o + Q_{2L}^{REFL} + Q_{4L}^{AD} + \ldots$

From Eq. (I-9), the value of q at x = L is

$$Q_L = Q_o \, e^{-\frac{\sqrt{3\alpha}}{D} L} \tag{I-12}$$

The value of Q_L^{AD} is obtained from the same argument used for Eq. (I-4) (or, in fact, Eq. (8)). Thus

$$Q_L^{AD} = \alpha \sqrt{\frac{RT}{2\pi M}} \, A P_L \tag{I-13}$$

where A is given by

$$A = \frac{\pi D^2}{4} \tag{I-14}$$

and P is obtained from Eq. (I-10). Thus

$$Q_L^{AD} = Q_o \, \frac{\sqrt{3\alpha}}{4} \, e^{-\frac{\sqrt{3\alpha}}{D} L} \tag{I-15}$$

The value of Q_L^{REFL} is obtained from

$$Q_L^{REFL} = Q_L - Q_L^{AD} = Q_o \, e^{-\frac{\sqrt{3\alpha}}{D} L} \left(1 - \frac{\sqrt{3\alpha}}{4}\right) \tag{I-16}$$

Now, repeating this chain of thought for x = 2L

$$Q_{2L} = Q_L^{REFL} \, e^{-\frac{\sqrt{3\alpha}}{D} L} = Q_o \left(1 - \frac{\sqrt{3\alpha}}{4}\right) e^{-\frac{\sqrt{3\alpha}}{D} L} \tag{I-17}$$

and

$$Q_{2L}^{AD} = \alpha \sqrt{\frac{RT}{2\pi M}} \, \frac{\pi D^2}{4} \, P_{2L} \tag{I-18}$$

where this time P_{2L} is given by Eq. (I-11). That is,

$$P_{2L} = \frac{\sqrt{3\alpha}}{D^2 \pi \alpha} \, \frac{Q_L^{REFL}}{\sqrt{\frac{RT}{2\pi M}}} \, e^{-\frac{\sqrt{3\alpha}}{D} L} \tag{I-19}$$

Therefore,

$$Q_{2L}^{AD} = Q_o \, \frac{\sqrt{3\alpha}}{4} \left(1 - \frac{\sqrt{3\alpha}}{4}\right) e^{-\frac{\sqrt{3\alpha}}{D} L} \tag{I-20}$$

And Q_{2L}^{REFL} follows in the same manner as Eq. (I-16). That is

$$Q_{2L}^{REFL} = Q_o \left(1 - \frac{\sqrt{3\alpha}}{4}\right)^2 e^{-\frac{2\sqrt{3\alpha}}{D} L} \tag{I-21}$$

By continuing this process for x = 3, x = 4, etc., it is easy to see that

$$Q_{nL} = Q_o \left(1 - \frac{\sqrt{3\alpha}}{4}\right)^{n-1} e^{-\frac{n\sqrt{3\alpha}}{D} L} \tag{I-22}$$

$$Q_{nL}^{AD} = \frac{\sqrt{3\alpha}}{4} Q_o \left(1 - \frac{\sqrt{3\alpha}}{4}\right)^{n-1} e^{-\frac{n\sqrt{3\alpha}}{D} L} \tag{I-23}$$

$$Q_{nL}^{REFL} = Q_o \left(1 - \frac{\sqrt{3\alpha}}{4}\right)^{n} e^{-\frac{n\sqrt{3\alpha}}{D} L} \tag{I-24}$$

Using Eq. (I-10) at x = 0,

$$Q_o + \sum_{n=1}^{\infty} Q_{2nL}^{REFL} = \frac{\alpha}{\sqrt{3\alpha}} D^2 \pi \sqrt{\frac{RT}{2\pi M}} \sum_{n=0}^{\infty} P_{2nL} \tag{I-25}$$

But $\sum_{n=0}^{\infty} P_{2nL}$ is just the measured pressure at x = 0, that is, P_1. Therefore,

$$Q_o \left[1 + \sum_{n=1}^{\infty} \left(1 - \frac{\sqrt{3\alpha}}{4}\right)^{2n} e^{-\frac{2n\sqrt{3\alpha}}{D} L}\right] = \frac{\alpha}{\sqrt{3\alpha}} D^2 \pi \sqrt{\frac{RT}{2\pi M}} P_1 \tag{I-26}$$

And summing up all equations such as Eq. (I-13) gives

$$Q_o^{AD} + \sum_{n=1}^{\infty} Q_{2nL}^{AD} = \alpha \sqrt{\frac{RT}{2\pi M}} \frac{\pi D^2}{4} \sum_{n=0}^{\infty} P_{2nL} = \alpha \sqrt{\frac{RT}{2\pi M}} \frac{\pi D^2}{4} P_1 \tag{I-27}$$

Recalling now that

$$Q_o^{AD} = Q - Q_o \tag{I-28}$$

Eq. (I-27) can be rewritten as

$$Q - Q_o + \frac{\sqrt{3\alpha}}{4} Q_o \sum_{n=1}^{\infty} \left(1 - \frac{\sqrt{3\alpha}}{4}\right)^{2n-1} e^{-\frac{2n\sqrt{3\alpha}}{D} L} = \alpha \sqrt{\frac{RT}{2\pi M}} \frac{\pi D^2}{4} P_1 \tag{I-29}$$

Solving Eq. (I-26) for Q_o, inserting that solution into Eq. (I-29), and then rearranging gives

$$\frac{Q}{P_1} = \alpha \sqrt{\frac{RT}{2\pi M}} \frac{\pi D^2}{4} \left\{1 + \sqrt{\frac{3}{\alpha}} \left[\frac{1}{1 + \sum_{n=1}^{\infty} e^{-2n\sqrt{3\alpha}\, L/D} \left(1 + \frac{\sqrt{3\alpha}}{4}\right)^{2n}}\right] - \left[\frac{\sum_{n=1}^{\infty} e^{-2n\frac{\sqrt{3\alpha}}{D} L} \left(1 - \frac{\sqrt{3\alpha}}{4}\right)^{2n-1}}{1 + \sum_{n=1}^{\infty} e^{-2n\sqrt{3\alpha}\, L/D} \left(1 - \frac{\sqrt{3\alpha}}{D}\right)^{2n}}\right]\right\} \tag{I-30}$$

In order to compare Eq. (I-30), which is identical with Eq. (9), to Eq. (8), it is convenient to plot the two equations, not as Q/P_1 as a function of α, but instead, P_1/Q as a function of α. A sketch of the behavior of these two equations (for the same temperature) is shown in Fig. 15d.

REFERENCES

1. Divatia, A. S. and Davis, R. H. "Construction and Performance of Evapor-Ion Pumps." Vacuum Symposium Transactions, Committee on Vacuum Techniques, Inc., 1954, p. 40.
2. Clausing, R. E. "A Large Scale Pumping Experiment Using Vapor Deposited Titanium Films." Transactions of the Eighth Vacuum Symposium and Second International Congress, Vol. 1, Washington, D. C., October 1961.
3. Kindall, S. M. and Wang, E. S. J. "Vacuum Pumping by Cryosorption." AEDC-TDR-62-183 (AD287182), October 1962.
4. Coogan, C. K. and Gutowsky, H. S. "Diffusion of Hydrogen in the Phase of Titanium Hydride." Journal of Chemical Physics, Vol. 36, No. 1, January 1962, pp. 110-116.
5. Emmett, Paul H. Catalysis, Vol. I. Reinhold Publishing Corporation, 1954.
6. Moore, W. J. Physical Chemistry. Prentice-Hall, Inc., 1959 (Second Edition).
7. Adamson, A. W. Physical Chemistry of Surfaces. Interscience Publishers, Inc., 1960.
8. Hickmott, T. W. "Interaction of Hydrogen with Tungsten." Journal of Chemical Physics, Vol. 32, No. 3, March 1960, pp. 810-823.
9. Ehrlich, G. and Hudda, F. G. "Direct Observation of Individual Adatoms: Nitrogen on Tungsten." Journal of Chemical Physics, Vol. 36, No. 12, June 1962, pp. 3233-3247.
10. Barrer, R. M. Diffusion in and through Solids. Cambridge University Press, 1959.
11. Dushman, S. Scientific Foundations of Vacuum Technique. John Wiley and Sons, Inc., 1962 (Second Edition).
12. Guthrie, A. and Wakerling, R. K. Vacuum Equipment and Techniques. McGraw Hill Book Company, 1949.

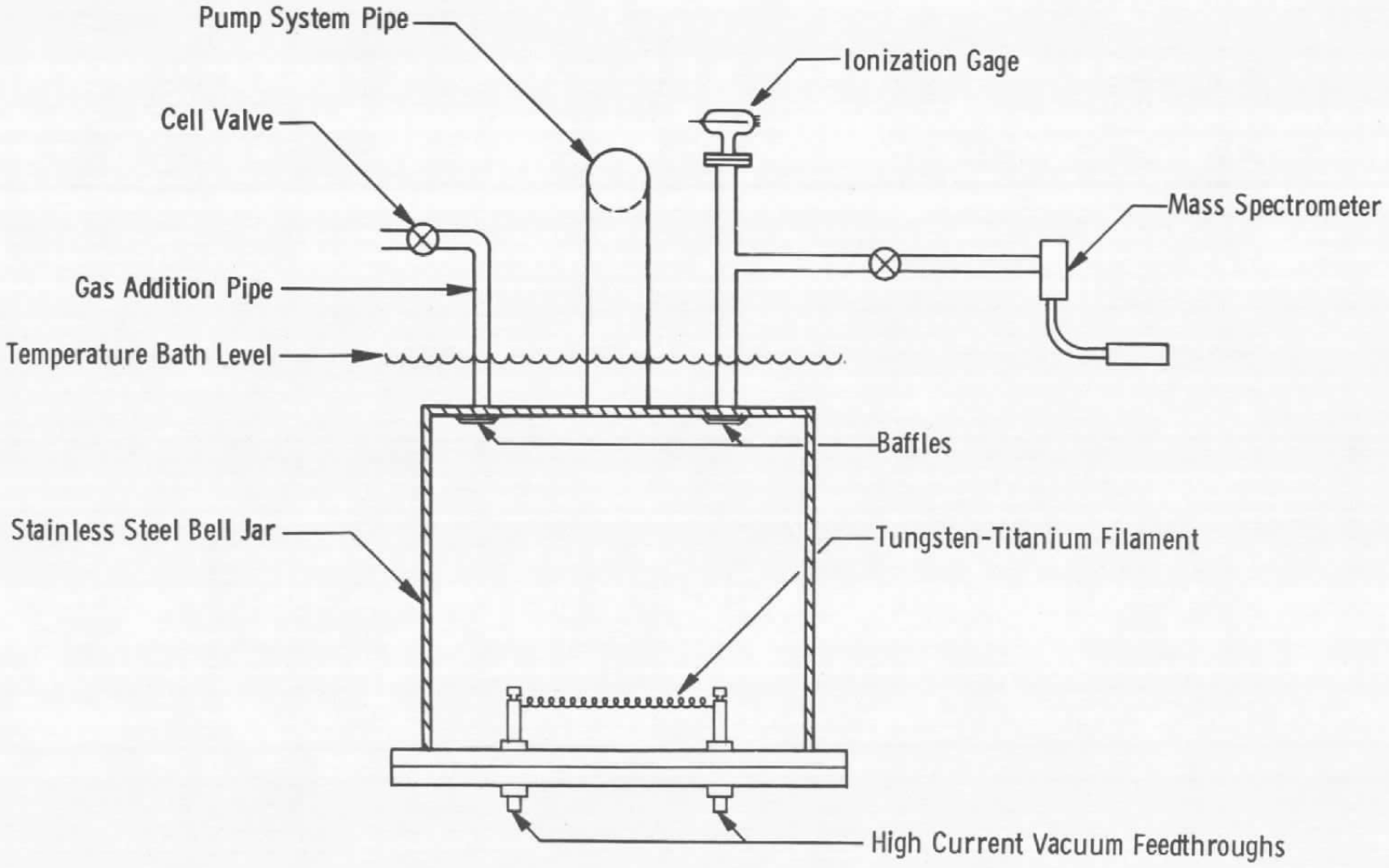

Fig. 1 Schematic of Vacuum Chamber

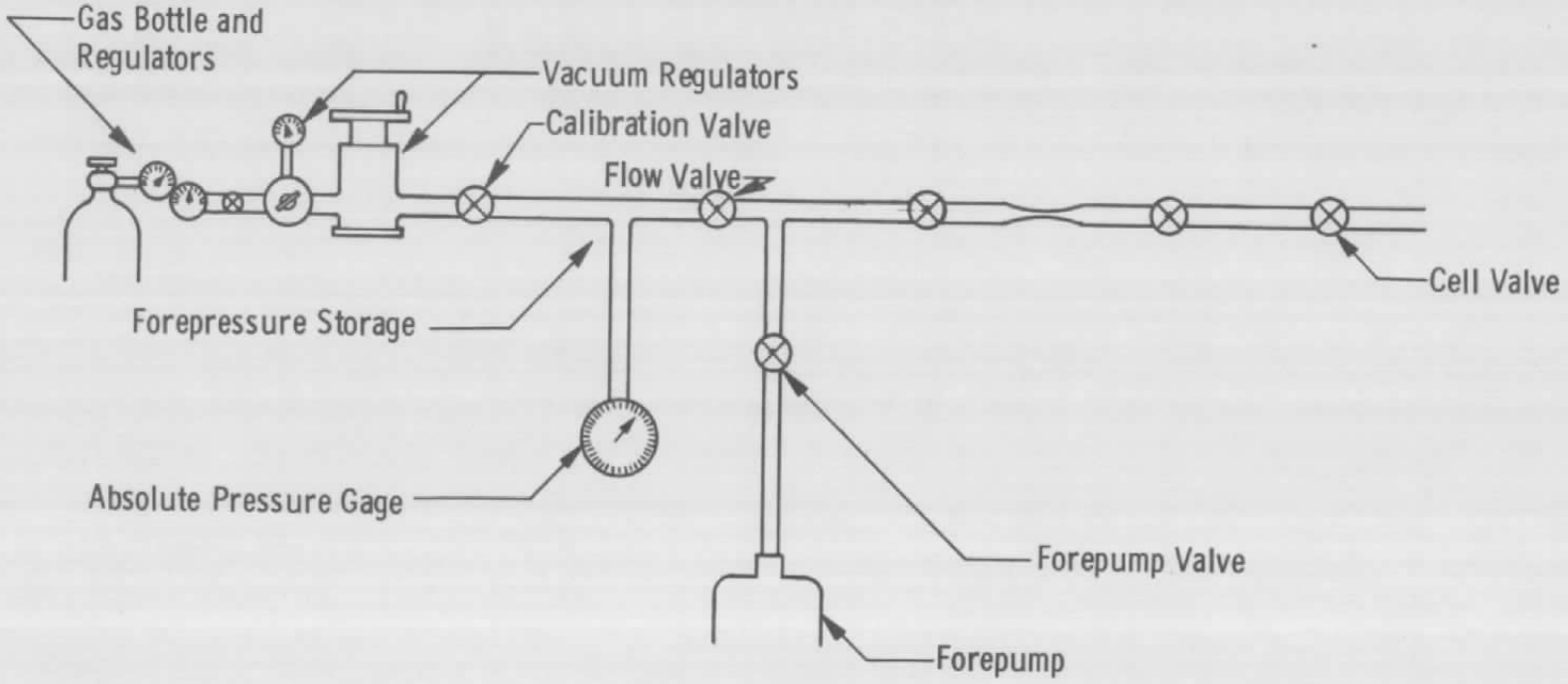

Fig. 2 Schematic of Gas Addition System

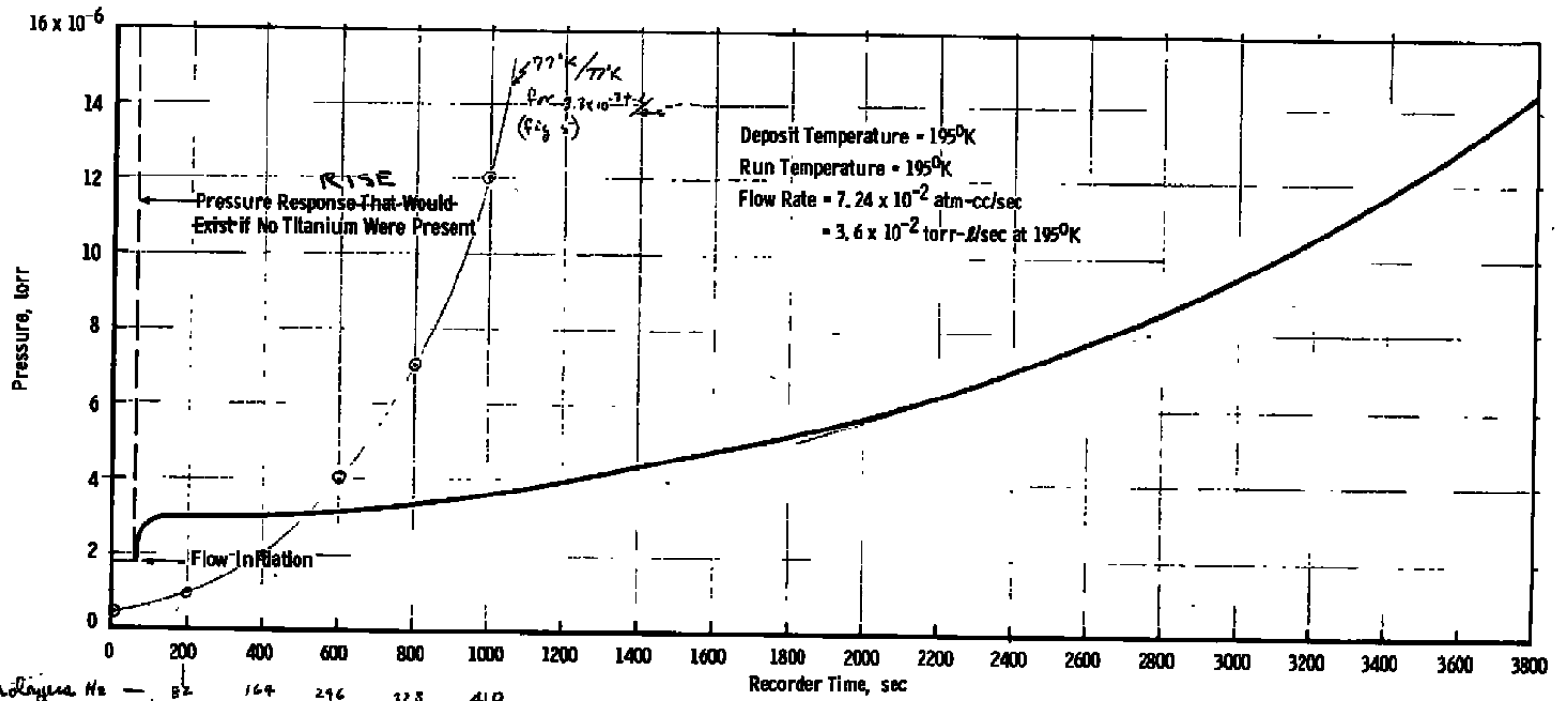

Fig. 3 Typical Pressure-Time Response

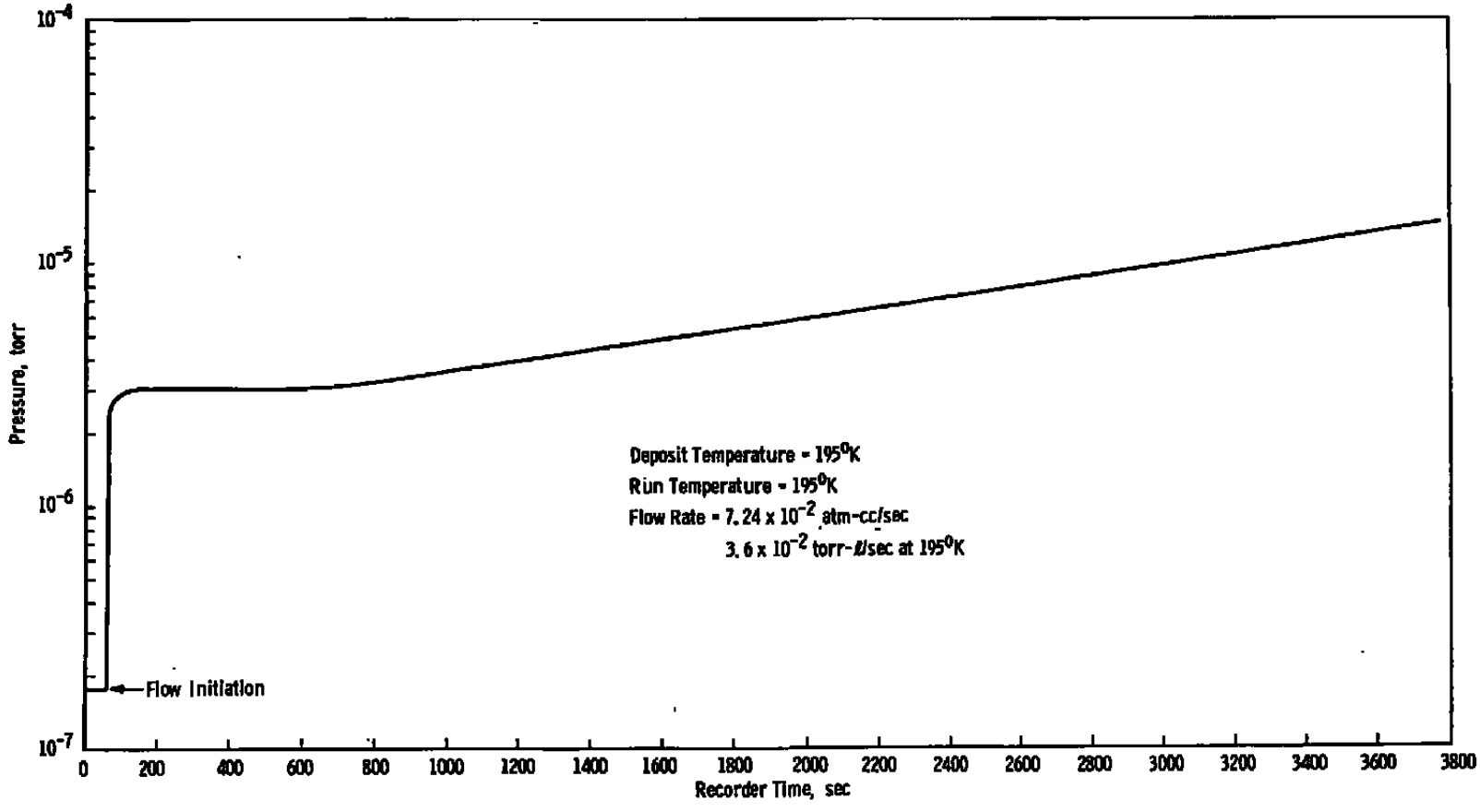

Fig. 4 Semilogarithmic Plot of a Typical Pressure-Time Response

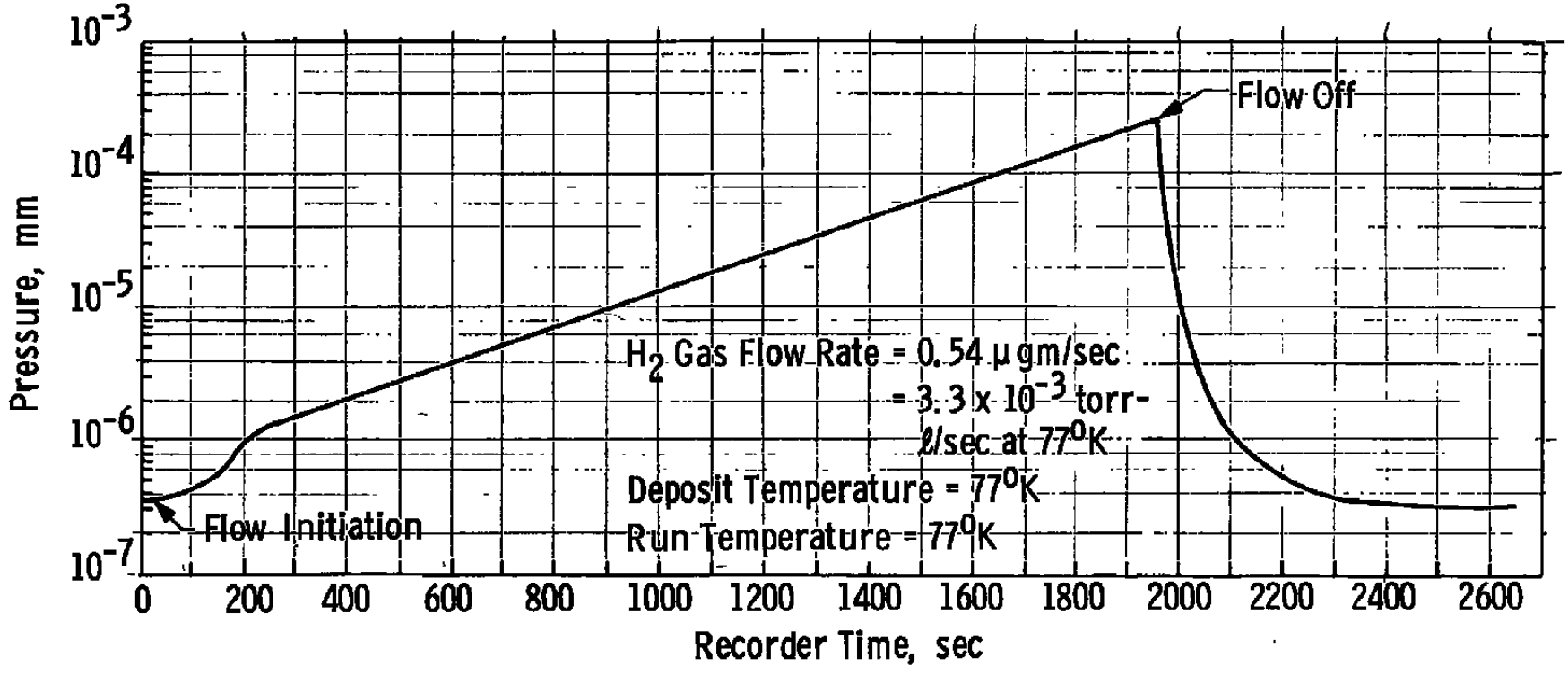

Fig. 5 Extended Typical Pressure-Time Response

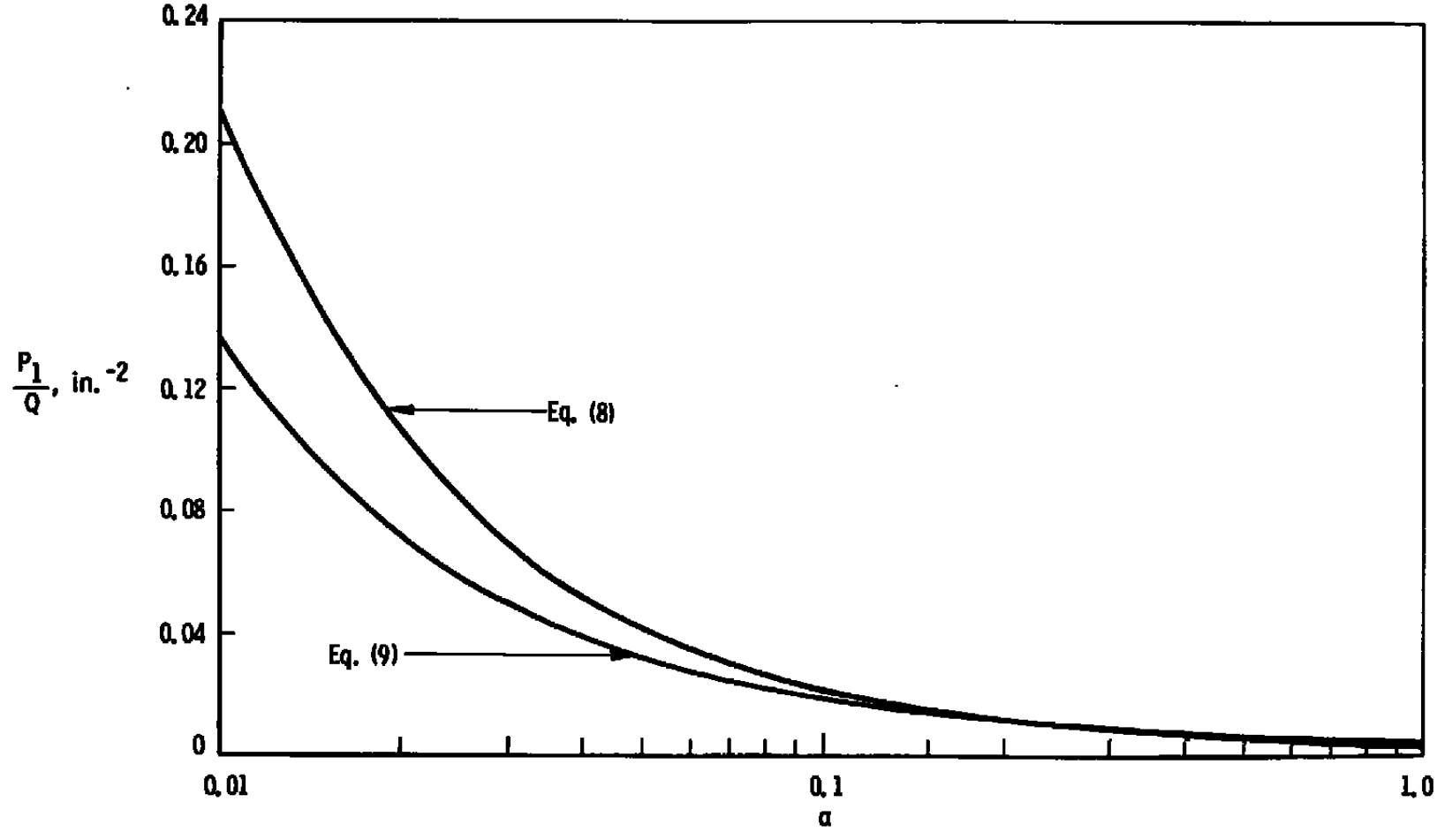

Fig. 6 P_1/Q for the Range of α from 0.01 to 1

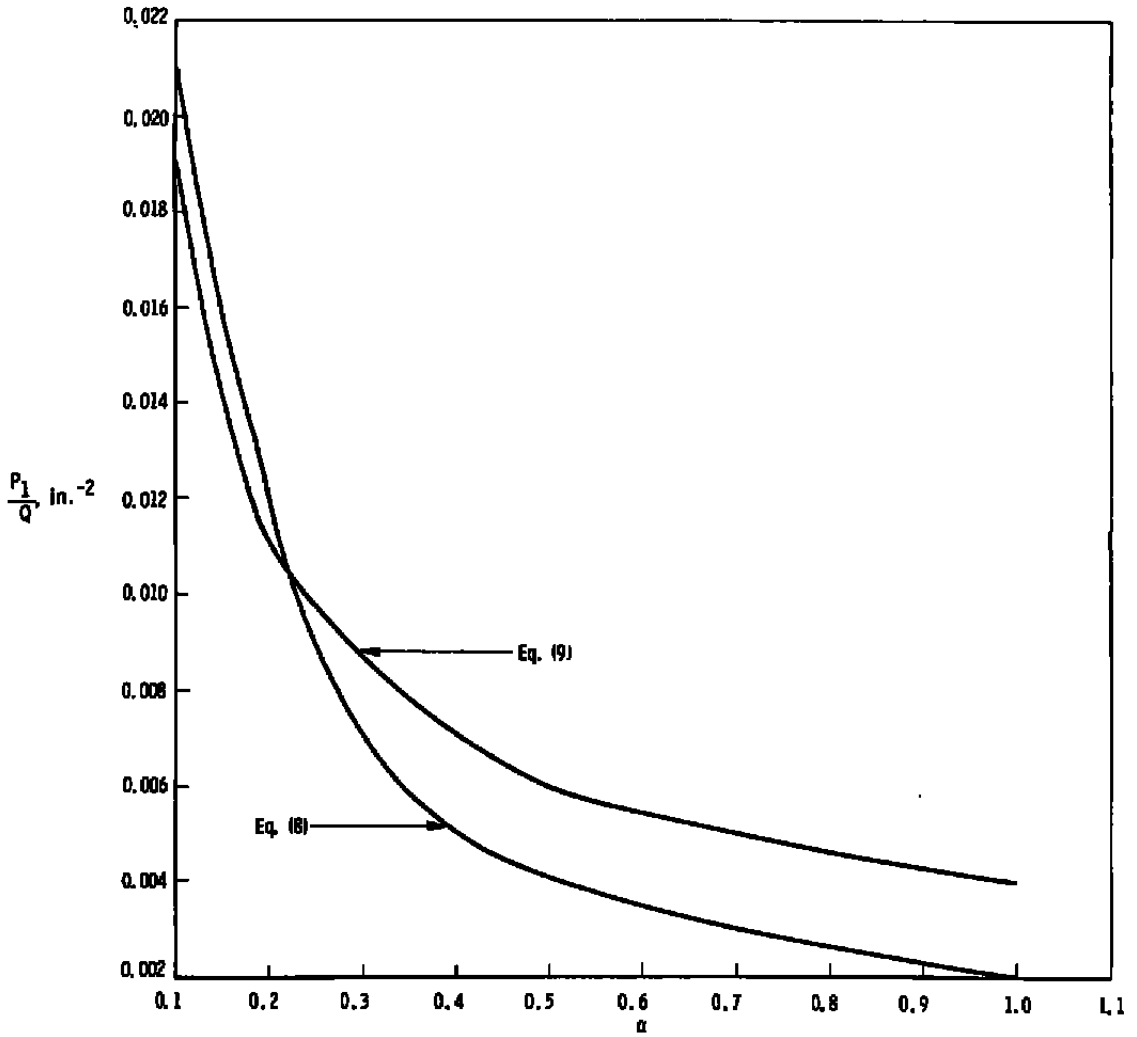

Fig. 7 P_1/Q for the Range of α from 0.1 to 1

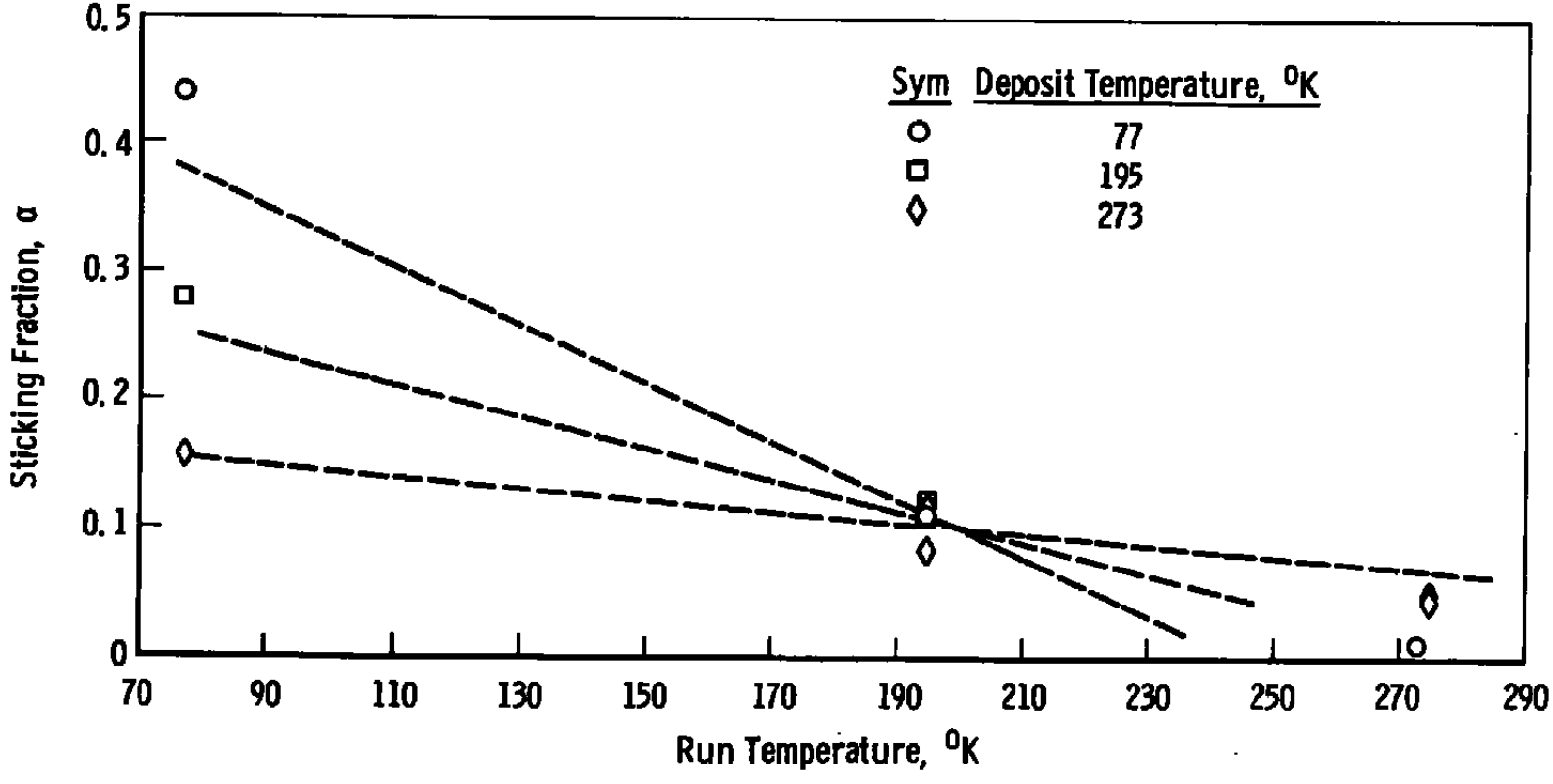

Fig. 8 Variation of Sticking Fraction with Run Temperature for Various Deposit Temperatures

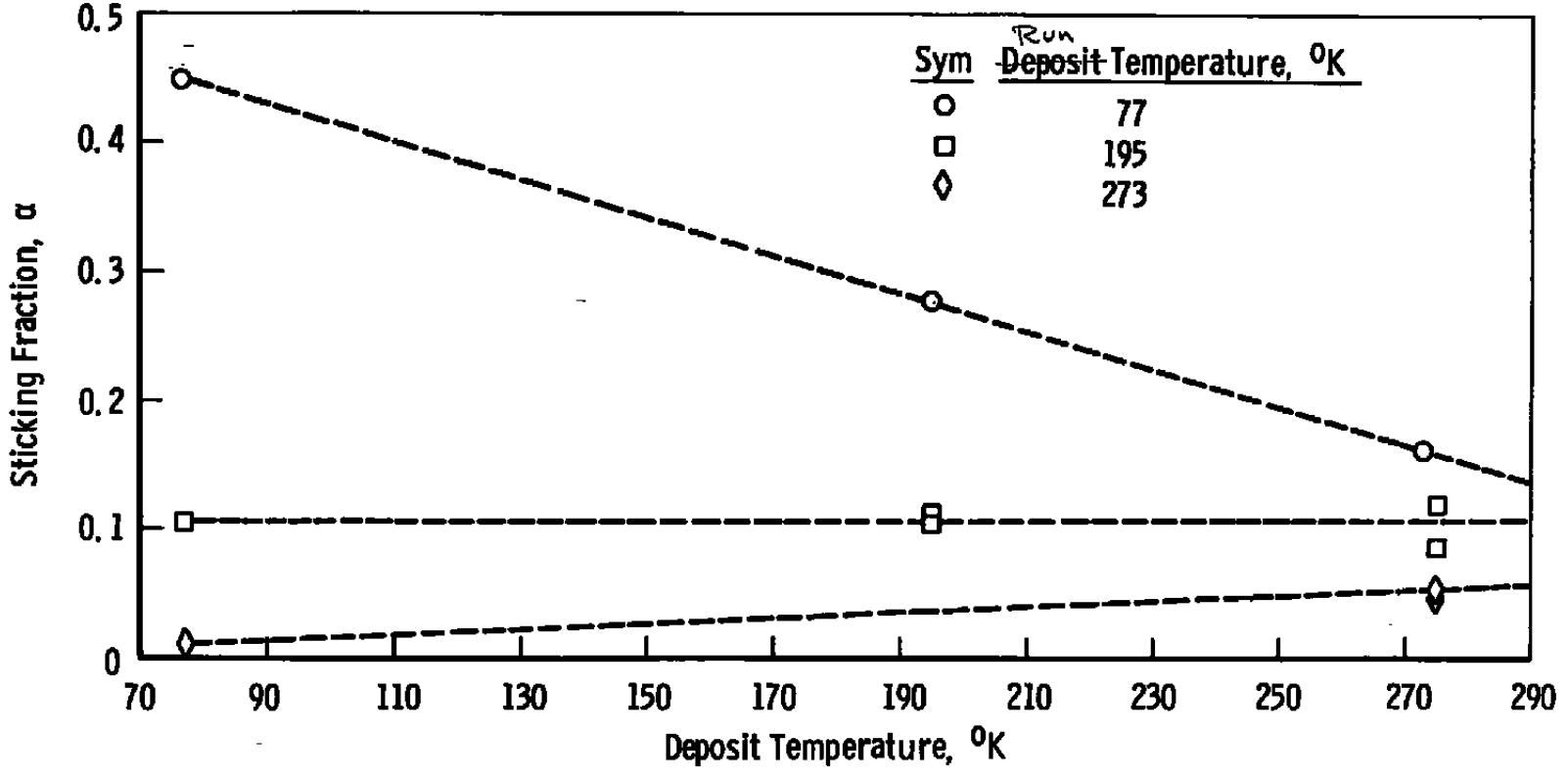

Fig. 9 Variation of Sticking Fraction with Deposit Temperature for Various Run Temperatures

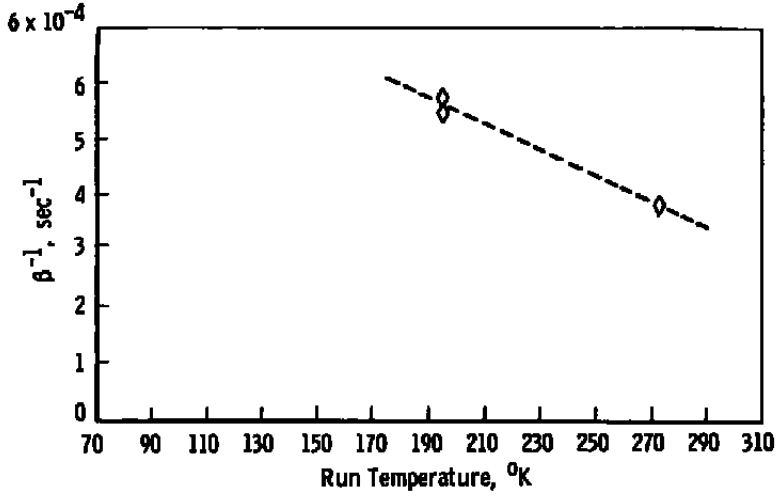

a. Deposit Temperature = 273°K

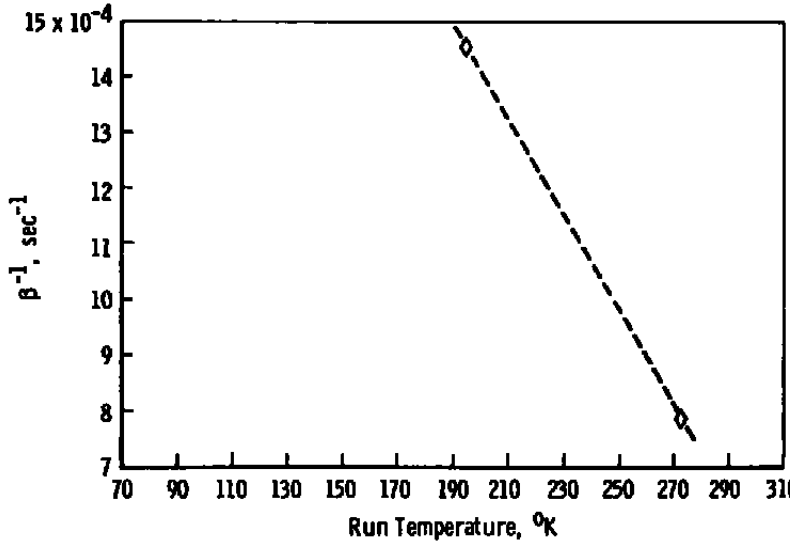

b. Deposit Temperature = 77°K

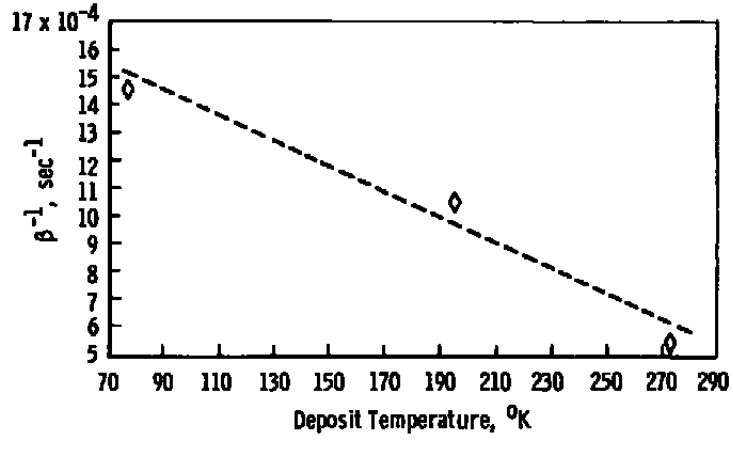

c. Run Temperature = 195°K

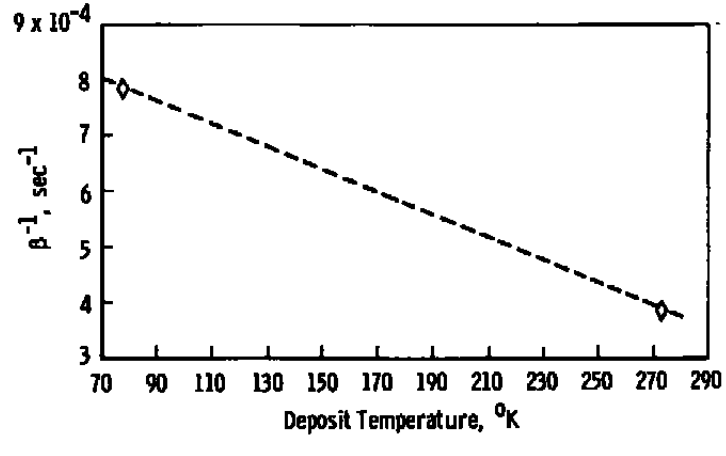

d. Run Temperature = 273°K

Fig. 10 Variation of the Reciprocal of the Exponential Decay Constant with Deposit and Run Temperature

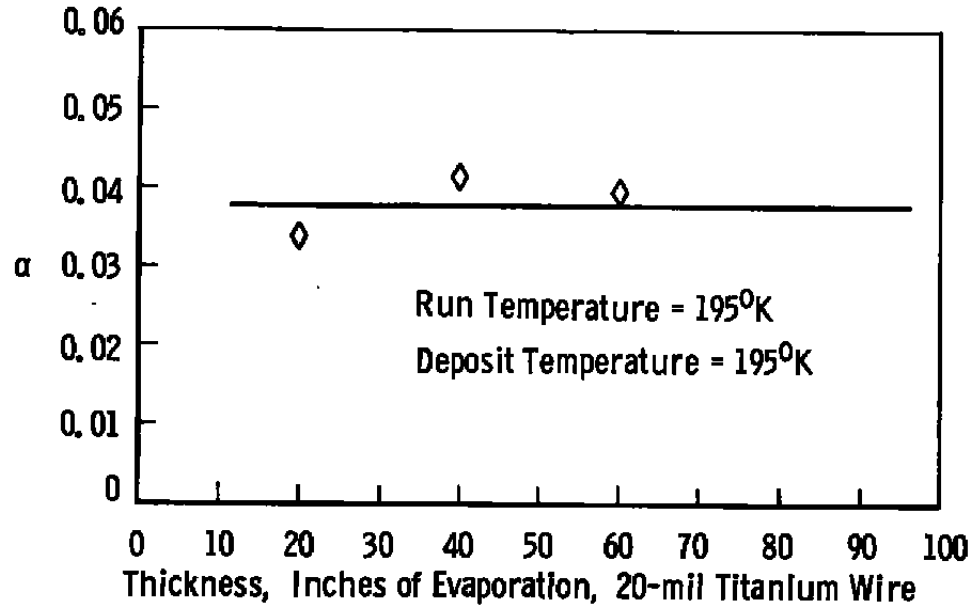

a. Sticking Fraction (α)

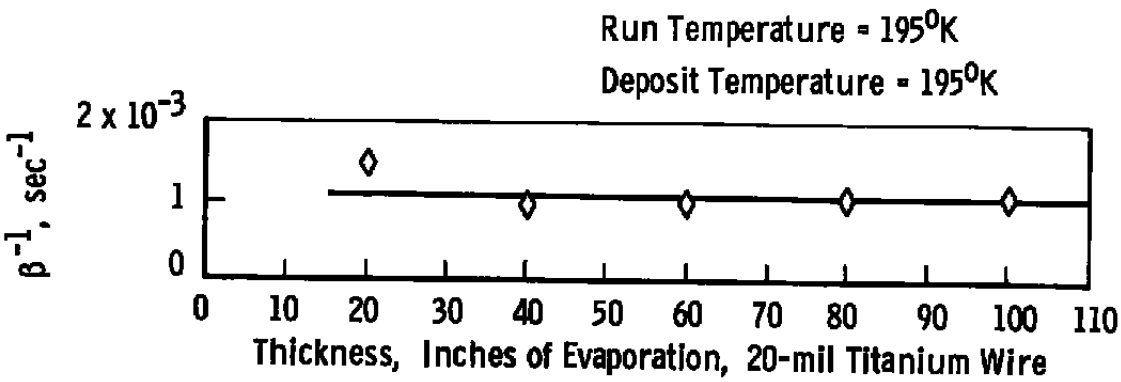

b. Reciprocal Decay Constant (β^{-1})

Fig. 11 Variation of Sticking Fraction and Reciprocal Decay Constant with Film Thickness

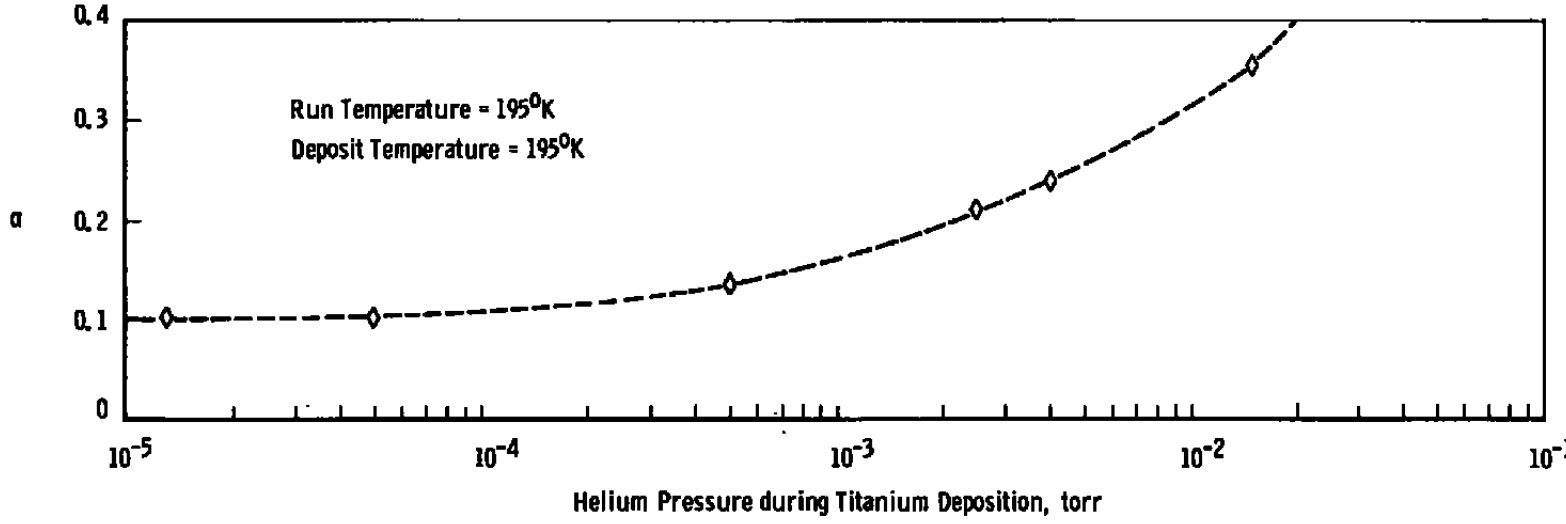

Fig. 12 Variation of Sticking Fraction with Chamber Helium Pressure during Deposition

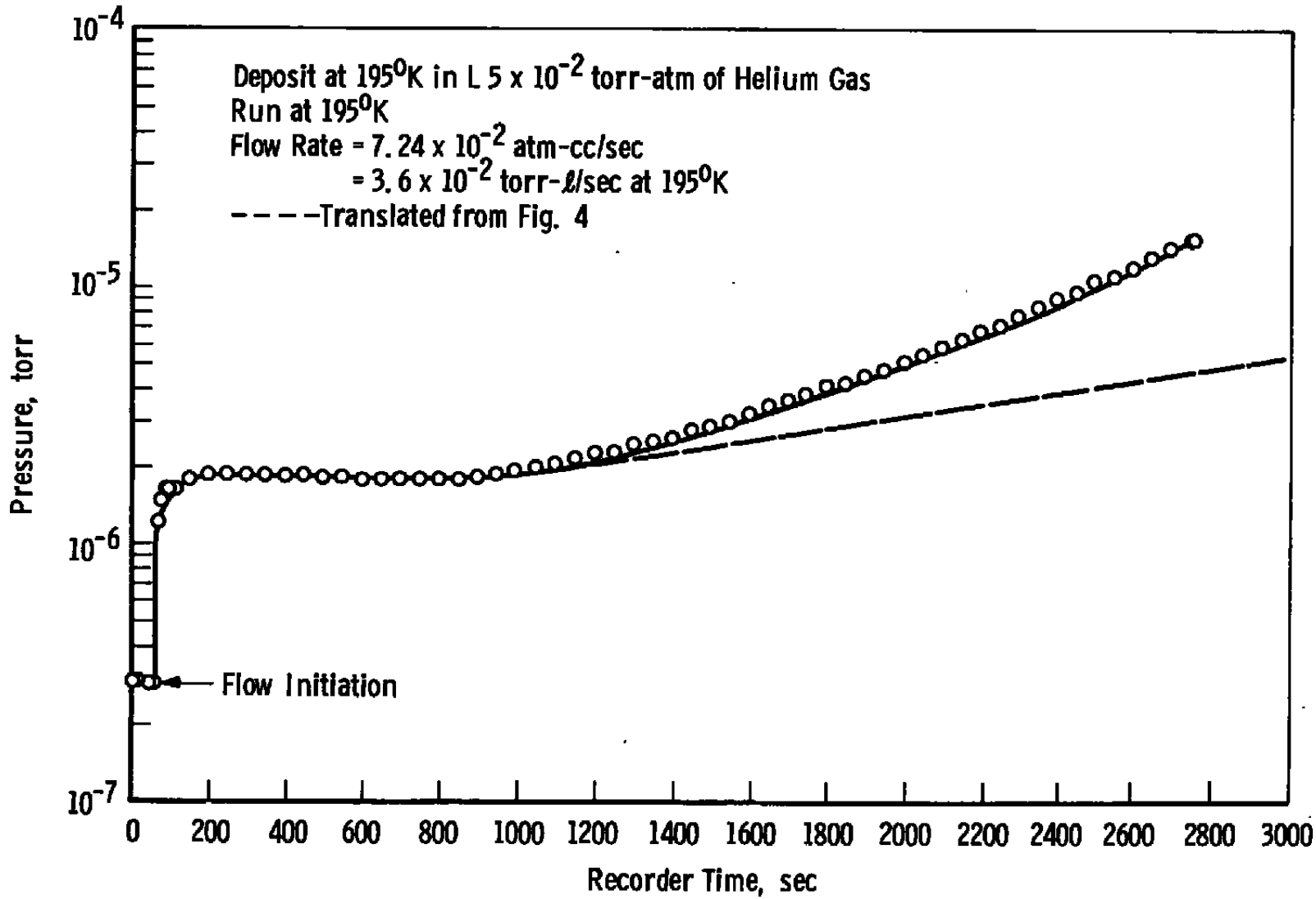

Fig. 13 Pressure-Time Response Due to Depositing Titanium within a Helium Atmosphere

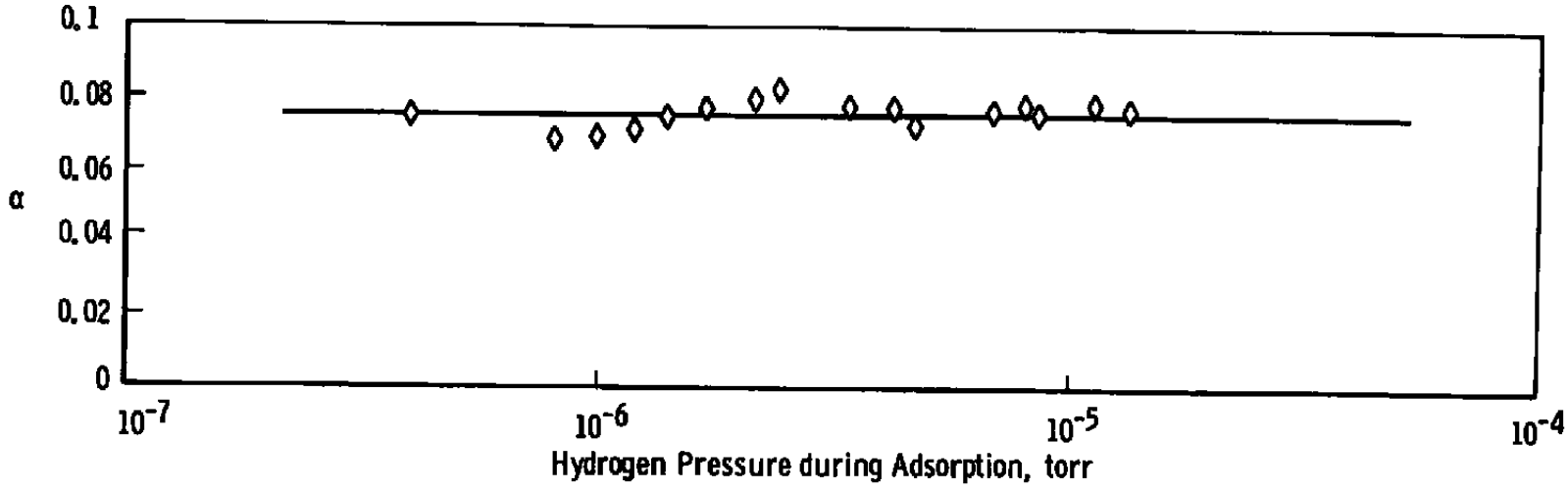

Fig. 14 Variation of Sticking Fraction with Chamber Pressure during Adsorption

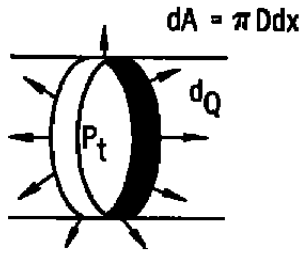

a. Adsorption by Incremental Ring

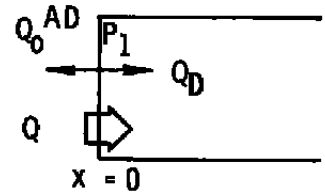

b. Adsorption of Throughput (Q)

P_1 = P at x = 0

Q_0^{AD} = Portion of Q Adsorbed at x = 0

Q = Throughput to Chamber

$Q = Q_0 + Q_0^{AD}$

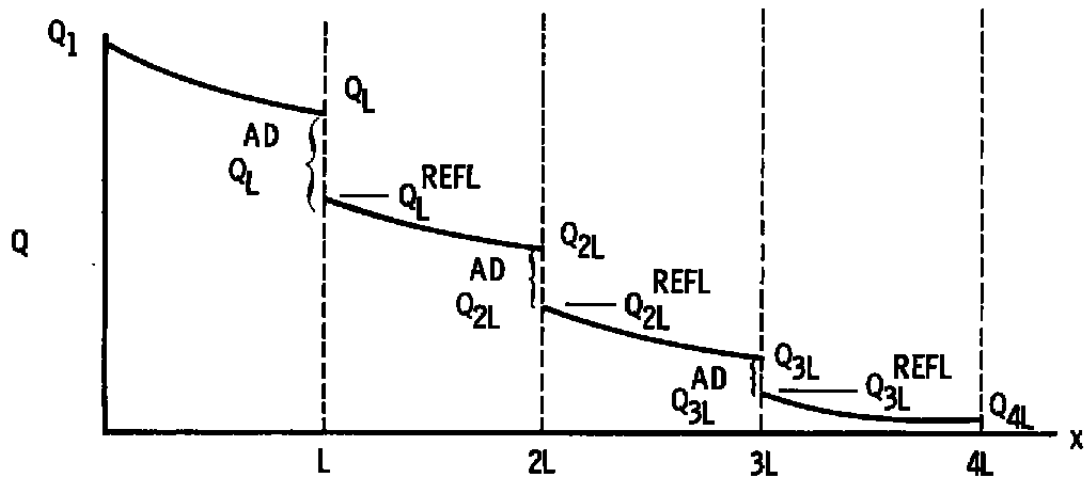

c. Adsorption of Throughput along the Length (L) of the Chamber

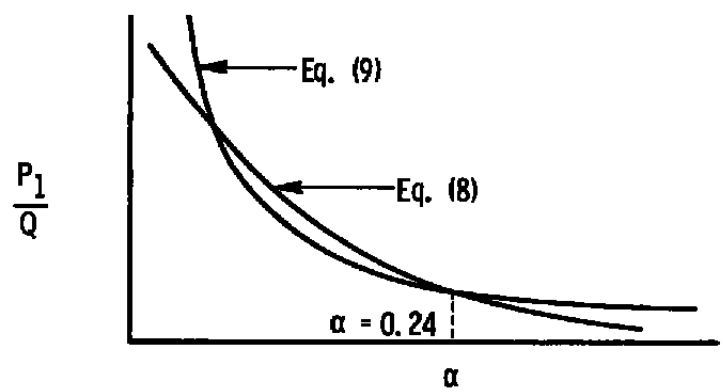

d. Comparison of Plots of P_1/Q as a Function of α Using Eqs. (8) and (9)

Fig. 15 Derivation Sketches for Eq. (9)

TABLE I
STICKING FRACTION AS A FUNCTION OF DEPOSIT TEMPERATURE FOR RUN TEMPERATURES OF 77°K

Deposit Temperature, °K	Run Temperature, °K	α Eq. (8)	α Eq. (9)	Specific* Pumping Speed, ℓ/sec-cm^2
77	77	0.45	0.84	18.9
195	77	0.28	0.375	8.4
273	77	0.16	0.14	3.14

TABLE II
STICKING FRACTION AS A FUNCTION OF HELIUM DEPOSIT PRESSURES FOR DEPOSIT AND RUN TEMPERATURES OF 195°K

Deposit Temperature, °K	Run Temperature, °K	Helium Dep. Pressure, torr	α Eq. (8)	α Eq. (9)	Specific* Pumping Speed, ℓ/sec-cm^2
195	195	1.3×10^{-5}	0.1	0.09	3.22
195	195	4×10^{-5}	0.102	0.092	3.3
195	195	5×10^{-5}	0.118	0.104	3.72
195	195	2.5×10^{-3}	0.214	0.2	7.16
195	195	4×10^{-3}	0.24	0.27	9.65
195	195	1.5×10^{-2}	0.358	0.55	19.7

*At run temperature using α from Eq. (9)

UNCLASSIFIED

Security Classification

DOCUMENT CONTROL DATA - R&D

(Security classification of title, body of abstract and indexing annotation must be entered when the overall report is classified)

1 ORIGINATING ACTIVITY *(Corporate author)*
Arnold Engineering Development Center
ARO, Inc., Operating Contractor
Arnold AF Station, Tennessee

2a REPORT SECURITY CLASSIFICATION
UNCLASSIFIED

2b GROUP
N/A

3 REPORT TITLE

ADSORPTION OF HYDROGEN BY A THIN FILM OF TITANIUM

4 DESCRIPTIVE NOTES *(Type of report and inclusive dates)*
N/A

5 AUTHOR(S) *(Last name, first name, initial)*

S. M. Kindall, ARO, Inc.

6 REPORT DATE	7a TOTAL NO. OF PAGES	7b. NO. OF REFS
August 1965	46	12

8a CONTRACT OR GRANT NO.	9a. ORIGINATOR'S REPORT NUMBER(S)
AF40(600)-1200 b. PROJECT NO. 8951 c. Program Element 61445014 d. Task 895104	AEDC-TR-65-113
	9b. OTHER REPORT NO(S) *(Any other numbers that may be assigned this report)* N/A

10. AVAILABILITY/LIMITATION NOTICES

Qualified requesters may obtain copies of this report from DDC.

11. SUPPLEMENTARY NOTES	12. SPONSORING MILITARY ACTIVITY
N/A	Arnold Engineering Development Center, Air Force Systems Command, Arnold AF Station, Tennessee

13. ABSTRACT

Past experience has shown that the capture coefficient of a titanium surface for hydrogen is strongly dependent upon the surface temperature and the conditions under which the film is formed. This report presents the results of an investigation which determined the importance of some of the variables. It was found that the capture coefficient increased as the titanium surface temperature was decreased from 273 to 77°K. Moreover, the capture coefficient could be further increased by lowering the temperature of the substrate upon which the titanium film was deposited from 273 to 77°K. Also, the capture coefficient was found to be independent of film thickness and chamber pressure but increased when the deposition was carried out in an inert helium atmosphere. For the range of conditions investigated, the sticking fraction was found to vary from 0.01 to 0.5. The experimental data suggest that surface diffusion is an important part of the mechanism by which titanium captures hydrogen. Calculations using a theoretical model which incorporates diffusion agreed well with the experimental results.

DD FORM 1 JAN 64 1473

UNCLASSIFIED

Security Classification

14 KEY WORDS	LINK A		LINK B		LINK C	
	ROLE	WT	ROLE	WT	ROLE	WT
hydrogen adsorption						
titanium						
capture coefficients						
thin films						
surface diffusion						
space simulation chambers						
diffusion pumps						
pressure						
temperature						
vacuum chambers						

INSTRUCTIONS

1. ORIGINATING ACTIVITY: Enter the name and address of the contractor, subcontractor, grantee, Department of Defense activity or other organization *(corporate author)* issuing the report.

2a. REPORT SECURITY CLASSIFICATION: Enter the overall security classification of the report. Indicate whether "Restricted Data" is included. Marking is to be in accordance with appropriate security regulations.

2b. GROUP: Automatic downgrading is specified in DoD Directive 5200.10 and Armed Forces Industrial Manual. Enter the group number. Also, when applicable, show that optional markings have been used for Group 3 and Group 4 as authorized.

3. REPORT TITLE: Enter the complete report title in all capital letters. Titles in all cases should be unclassified. If a meaningful title cannot be selected without classification, show title classification in all capitals in parenthesis immediately following the title.

4. DESCRIPTIVE NOTES: If appropriate, enter the type of report, e.g., interim, progress, summary, annual, or final. Give the inclusive dates when a specific reporting period is covered.

5. AUTHOR(S): Enter the name(s) of author(s) as shown on or in the report. Enter last name, first name, middle initial. If military, show rank and branch of service. The name of the principal author is an absolute minimum requirement.

6. REPORT DATE: Enter the date of the report as day, month, year; or month, year. If more than one date appears on the report, use date of publication.

7a. TOTAL NUMBER OF PAGES: The total page count should follow normal pagination procedures, i.e., enter the number of pages containing information.

7b. NUMBER OF REFERENCES: Enter the total number of references cited in the report.

8a. CONTRACT OR GRANT NUMBER: If appropriate, enter the applicable number of the contract or grant under which the report was written.

8b, 8c, & 8d. PROJECT NUMBER: Enter the appropriate military department identification, such as project number, subproject number, system numbers, task number, etc.

9a. ORIGINATOR'S REPORT NUMBER(S): Enter the official report number by which the document will be identified and controlled by the originating activity. This number must be unique to this report.

9b. OTHER REPORT NUMBER(S): If the report has been assigned any other report numbers *(either by the originator or by the sponsor)*, also enter this number(s).

10. AVAILABILITY/LIMITATION NOTICES: Enter any limitations on further dissemination of the report, other than those imposed by security classification, using standard statements such as:

(1) "Qualified requesters may obtain copies of this report from DDC."

(2) "Foreign announcement and dissemination of this report by DDC is not authorized."

(3) "U. S. Government agencies may obtain copies of this report directly from DDC. Other qualified DDC users shall request through _____."

(4) "U. S. military agencies may obtain copies of this report directly from DDC. Other qualified users shall request through _____."

(5) "All distribution of this report is controlled. Qualified DDC users shall request through _____."

If the report has been furnished to the Office of Technical Services, Department of Commerce, for sale to the public, indicate this fact and enter the price, if known.

11. SUPPLEMENTARY NOTES: Use for additional explanatory notes.

12. SPONSORING MILITARY ACTIVITY: Enter the name of the departmental project office or laboratory sponsoring *(paying for)* the research and development. Include address.

13. ABSTRACT: Enter an abstract giving a brief and factual summary of the document indicative of the report, even though it may also appear elsewhere in the body of the technical report. If additional space is required, a continuation sheet shall be attached.

It is highly desirable that the abstract of classified reports be unclassified. Each paragraph of the abstract shall end with an indication of the military security classification of the information in the paragraph, represented as *(TS), (S), (C), or (U)*.

There is no limitation on the length of the abstract. However, the suggested length is from 150 to 225 words.

14. KEY WORDS: Key words are technically meaningful terms or short phrases that characterize a report and may be used as index entries for cataloging the report. Key words must be selected so that no security classification is required. Identifiers, such as equipment model designation, trade name, military project code name, geographic location, may be used as key words but will be followed by an indication of technical context. The assignment of links, rules, and weights is optional.